University of California

Ernest O. Lawrence Radiation Laboratory

AN ELECTRONIC SCHEME FOR MEASUREMENT OF EXPLODING WIRE ENERGY

Livermore, California

UNIVERSITY OF CALIFORNIA

Lawrence Radiation Laboratory

Livermore, California

AEC Contract No. W-7405-eng-48

AN ELECTRONIC SCHEME FOR MEASUREMENT OF
EXPLODING WIRE ENERGY

R. J. Thomas

J. R. Hearst

July 7, 1965

AN ELECTRONIC SCHEME FOR MEASUREMENT OF
EXPLODING WIRE ENERGY

R. J. Thomas and J. R. Hearst

Lawrence Radiation Laboratory, University of California
Livermore, California

ABSTRACT

With the exception of a nuclear explosion itself, the highest energy density that can be obtained at a given point for a short time results from a wire explosion when a sudden large pulse of electrical current is passed through it. The energy (of the order of 8.5 kJ) in an exploding wire has been measured as a function of time by means of a scheme which, except for the sweep circuits of the oscilloscopes, uses only passive circuit elements and requires no calculated corrections for inductive effects. A shunt was placed in the transmission line to measure current, and a high-voltage resistive divider was placed across the wire to measure true resistive voltage. The divider was compensated for both the self-inductance of the wire and any mutual inductance of the divider and the circuit. The risetime responses of both measuring devices and all associated measurement circuit components were short compared to the risetime of the signals. The output values from the shunt and the divider were input into a computer program, which gave energy as a function of time from $\int ei\, dt$, where e is the true resistive voltage across the wire and i is the current through it. The energy values thus obtained compared favorably with those obtained from measurements of the shock wave in air caused by the wire explosion. Slow expansion of the wire as energy entered it, followed by rapid explosion, could be seen.

INTRODUCTION

In order to predict the effects of nuclear explosions in dense material, it is desirable to simulate such explosions in the laboratory on a small scale. Calculational techniques may thus be tested[1] and new models of behavior developed. In the past, high explosives have been used as an energy source for this work, but their energy density is orders of magnitude below that of nuclear explosives.

Next to a nuclear explosive itself, the highest energy density that can be obtained at a given point for a short time results from a wire explosion when a sudden large

---

[1] J. R. Hearst and L. B. Geesaman, Lawrence Radiation Laboratory (Livermore) Rept. UCRL-12065, October 1, 1964.

pulse of electrical current is passed through it. Energies of the order of 10 kJ are desired, deposited in a time of the order of 0.1 μsec. This energy must be known, as a function of time, with a reasonable degree of accuracy before the experiments can be interpreted quantitatively.

This report discusses an electronic energy-measurement scheme and exploding wire source devised by R. J. Thomas. The energy source is slower than ultimately required, but is applicable to the faster source when it becomes available.

Photography of shock waves from explosions in air was used to check the electronic measurements. The shock wave photography and data analysis were provided by J. R. Hearst.

Energy E(t) was obtained from $\int$ ei dt, where e is the instantaneous true resistive voltage (TRV) across the wire and i is the instantaneous current through it. The TRV component rather than the total voltage across the wire is required if one is to obtain energy as a function of time.

The principal measurement devices included a shunt inserted in the line to measure current and a resistive divider, compensated for inductance effects, to measure TRV. The combined risetime response of all elements comprising the current and voltage measuring circuits was always much shorter than that of the signals.

The most difficult part of this work is the actual measurement of the TRV, which obviates calculated corrections due to inductive effects. The present scheme represents a simplification of technique and circuitry compared to previous methods.[2,3] It lends itself to minimum equipment requirements and to greater convenience, accuracy, and freedom from spurious signals due mainly to complete use of coaxial passive circuit elements. It is applicable to both lumped-constant and traveling-wave exploders.

EXPERIMENTAL SETUP

The Circuit

Figure 1 shows the energy discharge circuit and associated measurement circuits exclusive of the time-mark system. The four 14.5 μF capacitors, connected by flat plates, stored 11.6 kJ at 20 kV. Thirty cables in parallel fed a flat-plate transmission line. The wire was held in movable jaws at the end of the line. Circuit inductance exclusive of the wire holder loop was 0.06 μH, and the loop inductance was 0.20 μH for 7.5-cm wires. Circuit resistance was 0.015 Ω, measured dynamically during the first cycle of a ringing discharge, increasing to 0.025 Ω during the fourth cycle.

[2]K. G. Moses and Theodore Korneff, Rev. Sci. Instr. 34 No. 8 (1963).

[3]S. W. Zimmerman, "Measurement of Surge Voltage in High Current Circuits," IEEE Conference Paper 64-154.
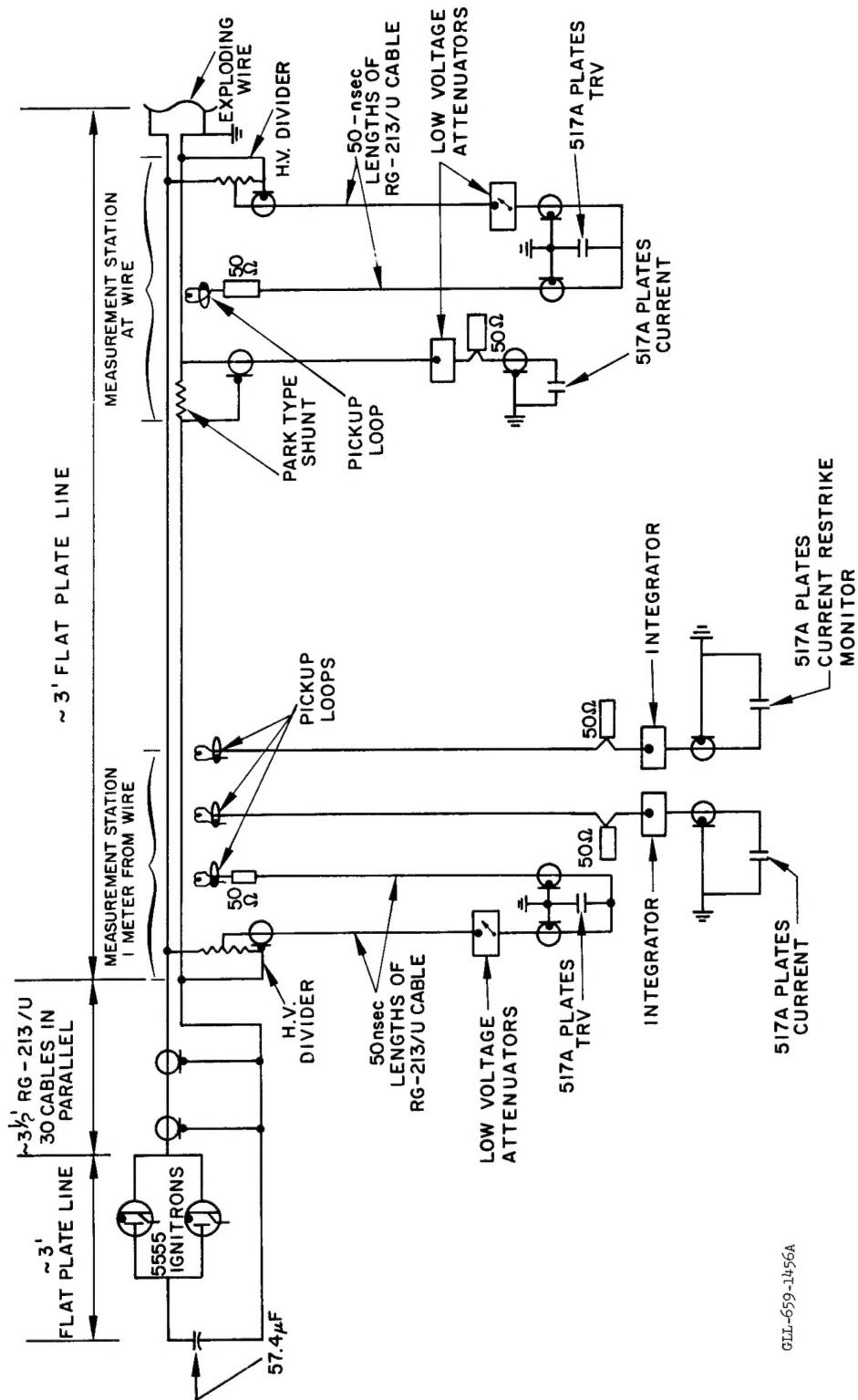
Fig. 1. Energy discharge circuit with associated measurement circuitry.

Experiments were performed in a large aluminum water tank. The flat-plate line went down the side of the tank and projected horizontally into the center. It could be slid vertically over a 25-cm travel for photographic purposes.

A horizontal third plate, attached to the grounded tank, supported the flat-plate line, but was insulated from it except at one end of the wire. The rest of the bank circuit was fully insulated from ground, eliminating ground loops.

In general, the bank circuit had lumped-constant, transient-response character-istics of a damped or overdamped series R-L-C circuit. However, to allow for traveling surges having fronts on the order of or less than the transit time of the line, the surge impedance of the low-voltage side (bottom plate) of the flat-plate line, with respect to the ground plane, was kept considerably smaller than that of the high-voltage side (top plate). Thus, the low-voltage side remained as close as possible to ground reference during surges, eliminating the need for differential voltage measurements with respect to ground either in the case of current shunts inserted in that side or for voltage sensors attached across the line. This condition was accomplished by keeping the bottom plate close to both the grounded tank wall and third plate and making it wider than the top plate. Both sides were tapered from their input end toward the wire end, the top plate tapering from 30 to 15 cm while the bottom plate extended beyond the top plate with a uniform 10 cm margin on both sides. Mylar was used for line insulation and for insulation from the ground plane with approximately a 7 cm flashover projection beyond all edges. No problems arose due to water immersion.

The flat-plate line accommodated a Park-type current shunt in the bottom plate 28 cm from the wire. A transverse slot was located in the bottom plate at the input end and another near the wire to accept pickup loops. High-voltage dividers were attached to the flat-plate line at the input end and at the wire end. The construction details of the line and the sensing devices are covered in the appendix.

ENERGY MEASUREMENT TECHNIQUE

Current Measurement

Current was measured primarily with the Park-type shunt.[4,5] Its output signal was fed through a length of 50 Ω cable and attenuated just before the signal was applied directly to the vertical deflection plates of an oscilloscope cathode ray tube (CRT) terminated in 50 Ω.

The integrated signal from a calibrated pickup loop was used as a second means of measuring current. Another such integrated loop signal was monitored at a much

---

[4] J. H. Park, J. Res. NBS (Research Paper RP 1823) **39**, (1947).

[5] Manufactured by T & M Research Products, Albuquerque, New Mexico; Model K-5000-8, R = 0.001 Ω, L = 0.01 μH, T_R = 36 nsec, 5000 J safe pulse dissipation.

longer sweep to verify absence of restrikes. Integrated signals from pickup loops were also applied directly to the deflection plates of the oscilloscope CRT.

True Resistive Voltage Measurements

The scheme of TRV recording reported here basically follows the same underlying principles as outlined in Ref. 2. The essential difference is that this scheme employs simpler circuitry based only on passive elements to compensate for errors due not only to any voltage mutually induced into the voltage sensor but also due to the self-inductance component of voltage drop across the wire. This result is achieved by cancelling these two "inductance" type voltages by means of an equal but 180° out-of-phase voltage derived from a pickup loop near the wire, leaving only the TRV component of the voltage sensor output to be recorded.

A high-voltage coaxial resistive divider was connected across the circuit about 15 cm from the wire. Its output was fed through a length of 50 Ω cable and further attenuated by low-voltage variable turret attenuators[6] (course and fine in series) located just ahead of the vertical deflection plates of an oscilloscope CRT. No terminating resistor was applied at the plates, but rather a second 50 Ω cable of the same length was connected in parallel with the plates, with a pickup loop at its far end. This loop was in a slot in the bottom side of the transmission line, near the wire.

During a discharge, signals from divider and loop, traveling equal cable lengths, arrive simultaneously at the oscilloscope plates. Since the unterminated oscilloscope plates are just tapped off the end of each cable, a 50 Ω impedance continuity is maintained as seen looking from the end of each cable into the opposite cable. This arrangement allows each signal to continue undisturbed past the plates into the opposite cable. The superposition of the two incident signals at the plates results in their algebraic addition. However, each incident signal must see an effective 50 Ω termination at the end of the opposite cable to prohibit reflections. Therefore, the divider was made to appear as a 50 Ω termination for the loop signal and the loop made to appear as a 50 Ω termination for the divider signal. Detail design and performance characteristics of the dividers and loops for this scheme are discussed in the appendix.

This measurement scheme is adjusted for response only to TRV by replacing a wire with a copper rod dummy. The rod should have the same length as a wire and be large enough in diameter to serve as a nonexploding, nonresistive inductance. In this case, the length of the rod was 7.5 cm and the diameter was 0.5 cm. The turret attenuators are then adjusted to obtain a straight line null on the oscilloscope when the bank is discharged through the dummy. The null can be adjusted most accurately during

---

[6]Manufactured by Telonic Industries, Beech Grove, Indiana; Model TB-50, 0 to 10 dB in 1-dB steps and Model TC-50, 0 to 1 dB in 0.1-dB steps, both having bandwidth dc to 1000 Mc/sec.

dummy discharges at the highest charge voltage anticipated for exploding wire discharges, because any unbalance will give a more pronounced departure from a straight line at higher discharge currents.

The turret attenuators were actually used in series with some additional fixed attenuators, all attenuators being of the coaxial T pad type to preserve a 50 Ω appearance in either direction when the output in either direction appears as 50 Ω.

Figures 2(a) and 2(b) show the divider and loop signals, respectively, during a null adjustment with a dummy load. Figure 2(c) shows the null achieved by electronic cancellation of the signals of Figs. 2(a) and 2(b). A perfect straight line null was never achieved, for the possible reasons discussed in the appendix. The null adjustment was fairly insensitive to dummy diameters covering the range of exploding wire expansion during energy deposition.

Time Measurement

Signals from a fiducial-mark generator and a time-mark generator were mixed and parallel fed from a cable fanout. They were introduced into the data signal systems through isolation resistors at the plates of each scope. Such a mismatched time-mark system can not be used with fast exploders, but is satisfactory at these speeds. The details of the timing system are covered in the appendix.

Typical Signals

Typical current and TRV waveforms from wire explosions in air are shown in Fig. 3. Figures 3(c) and 3(d) show an optimum condition at a bank charge voltage of 17.9 kV, in which the wire accepted energy in one unipolarity overdamped current pulse without restrikes. There was a slight current reversal after the main pulse.

Figure 4(a) shows the uncompensated divider signal for such an explosion, and Fig. 4(b), the loop signal; the two combine to form Fig. 3(d).

Signals for a wire exploded at a bank charge voltage of 9.0 kV are shown in Fig. 5. The absence of a pronounced voltage spike and the smoothly ringing current are characteristic of insufficient energy to produce a strong explosion.

Figure 6 demonstrates the contrast between a wire exploded in air and one in water, both at a bank charge voltage of 22 kV. Figures 6(a) and 6(b) are for an explosion in air. The bank energy was more than the wire could accept, as shown by the ringing after an overdamped current interval ending at the break in the decline from the first current peak. Figures 6(c) and 6(d) are for a similar explosion in water. The containment by the water caused the wire to accept energy in one unipolarity overdamped current pulse.
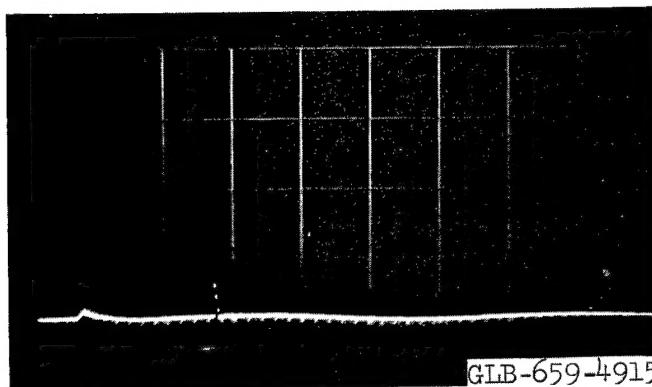
This energy measurement scheme allows voltage divider measurements or current shunt measurements at any point on the energy discharge circuit providing that the low side of the circuit at the point in question does not jump during the discharge more than
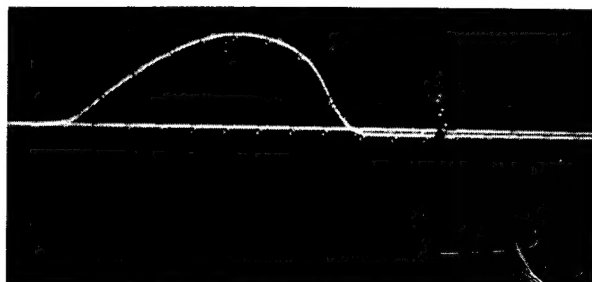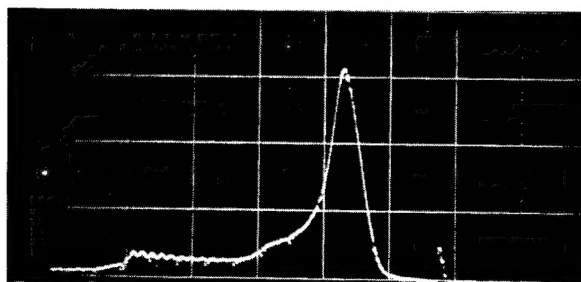
-7-
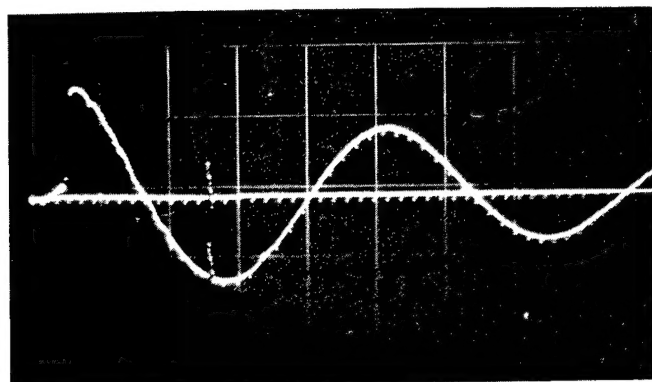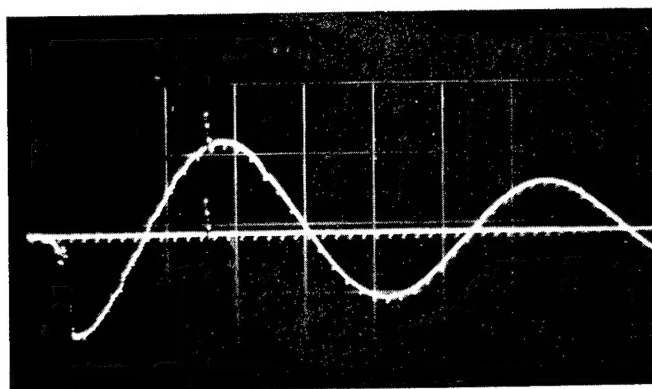
Fig. 2 (a) Uncompensated voltage divider signal with dummy load.
(b) Pickup loop signal with dummy load. (c) "Straight line" sum of (a) and
(b) with dummy load. Time marks 1 μsec apart.

Current on left   Voltage on right

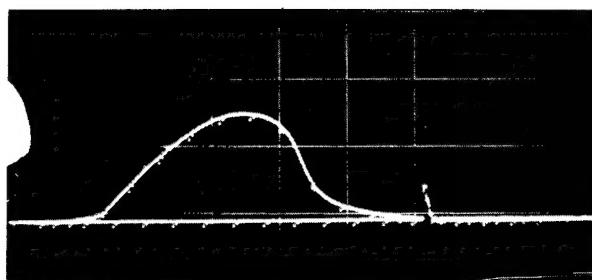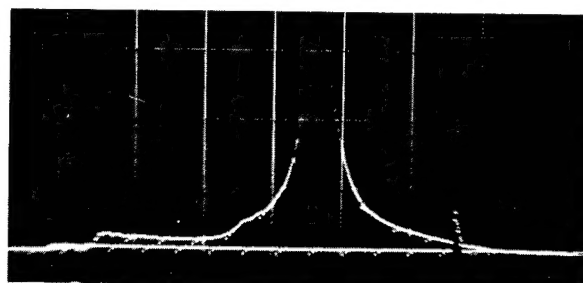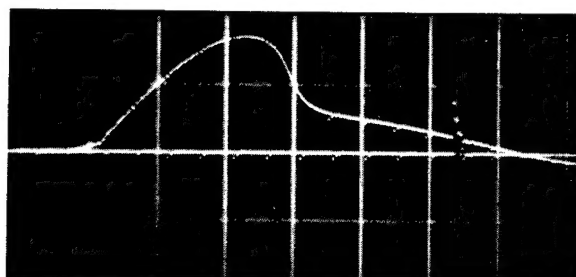(a)   (b)
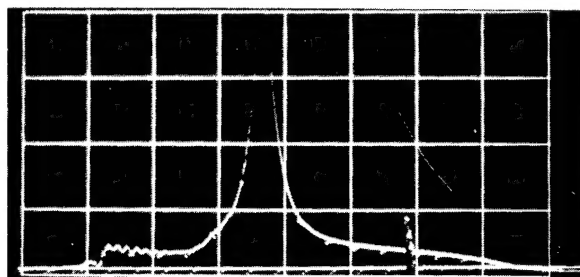
Shot 40, 15.3 kV in air

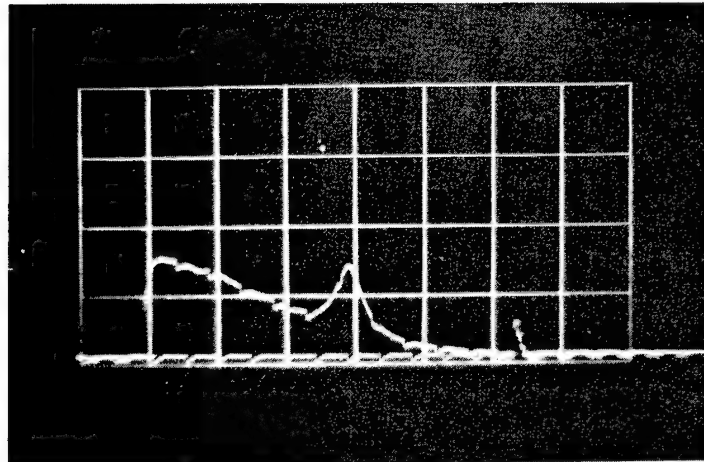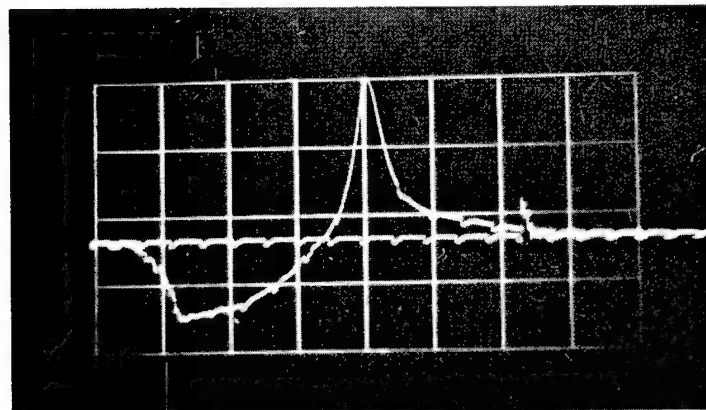(c)   (d)

Shot 47, 17.9 kV in air

(e)   (f)   GLB-659-4916

Shot 31, 20.6 kV in air

Fig. 3. Current and voltage signals from three shots with different bank
charge voltages. Time marks 1 μsec apart.

(a)

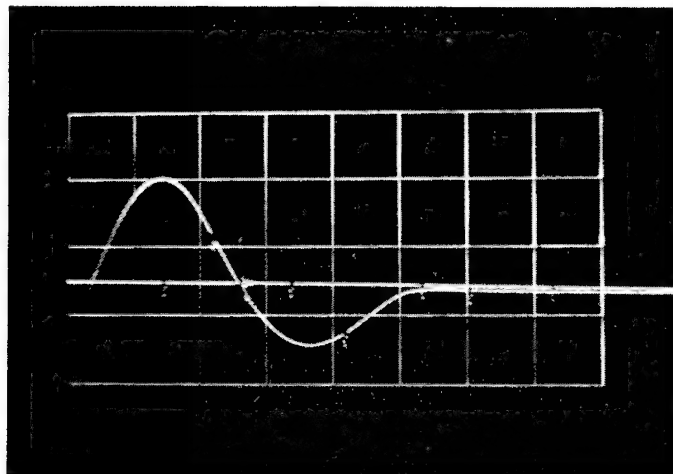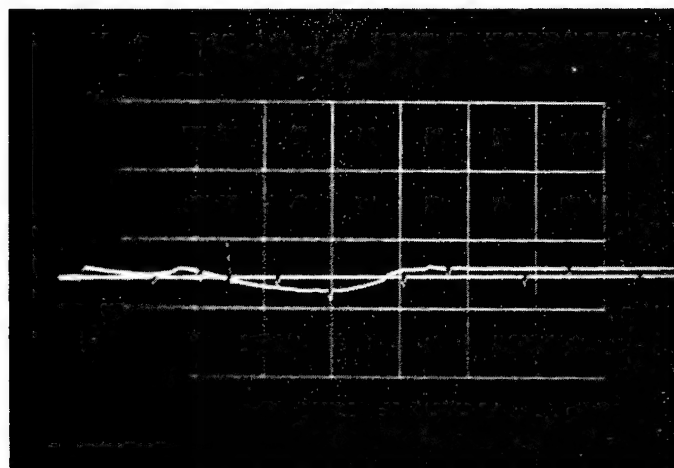Uncompensated voltage divider signal

(b)   GLB-659-4917

Pickup loop signal

Fig. 4. Signals from wire explosion in air with 17.9 kV bank charge
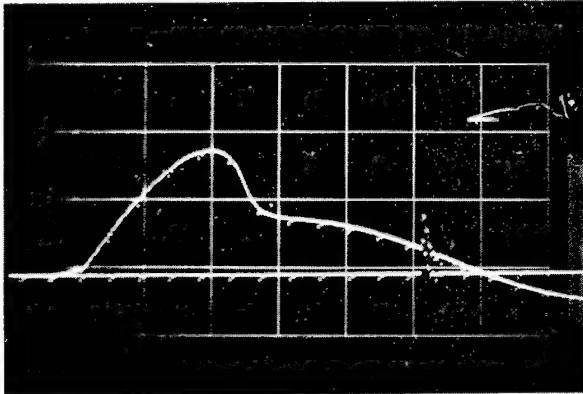voltage.   Time marks 1 μsec apart.

(a)

Current

(b)   GLB-659-4918

Voltage

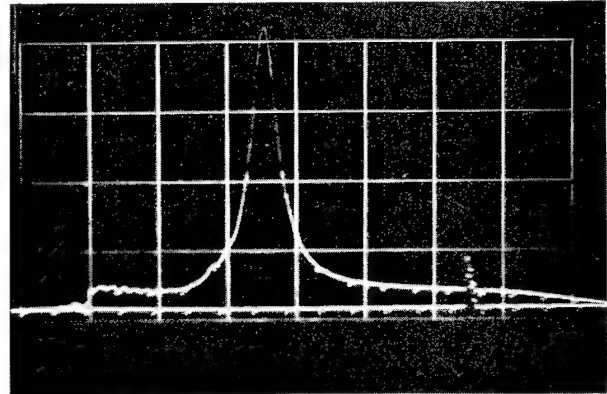Fig. 5. Signals from wire explosion in air with 9 kV bank charge voltage. Time marks 10 μsec apart.
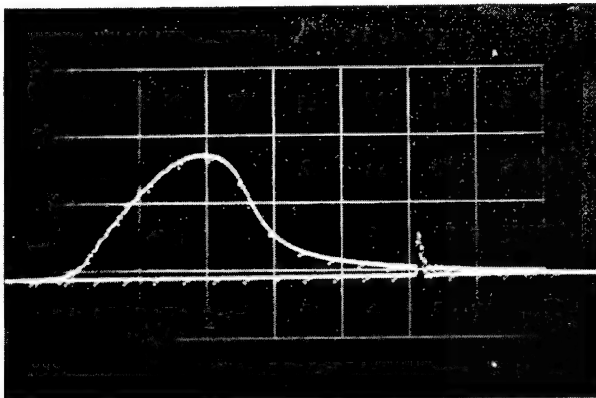
Current on left   Voltage on right
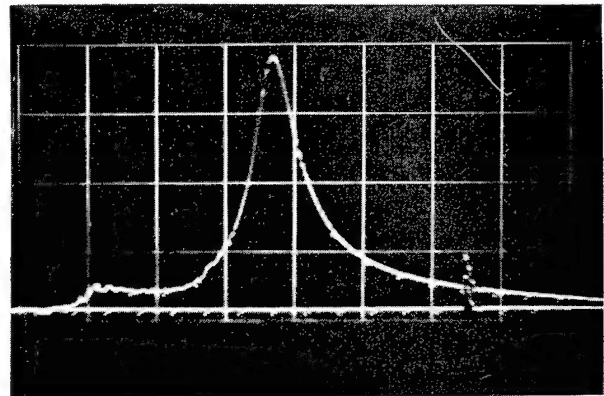

(a)   (b)

22 kV in air

(c)   (d)   GLB-659-4919

22 kV in water

Fig. 6. Signals from wire explosion in air and in water with same bank charge voltage. Time marks 1 μsec apart.

about 1000 V above the power supply ground of measurement oscilloscopes having signals fed directly on the plates. Current measurements with calibrated pickup loops which are fully insulated can be made at any point on the energy discharge circuit.

The above paragraph applies only to situations for which the risetime of the energy discharge pulse is considerably longer than the transit time through the energy discharge circuit. When the risetime is less or of the order of the transit time, such as in fast impedance-matched wire exploders, measurements can be made only immediately adjacent to the wire.

In the case reported here, current and voltage were measured adjacent to the wire and at 1 m "upstream" from the wire. Measured energies at these locations agreed within ±10%. The error was due mainly to poor picture quality on the upstream oscilloscopes. Figure 7 compares current and voltage.
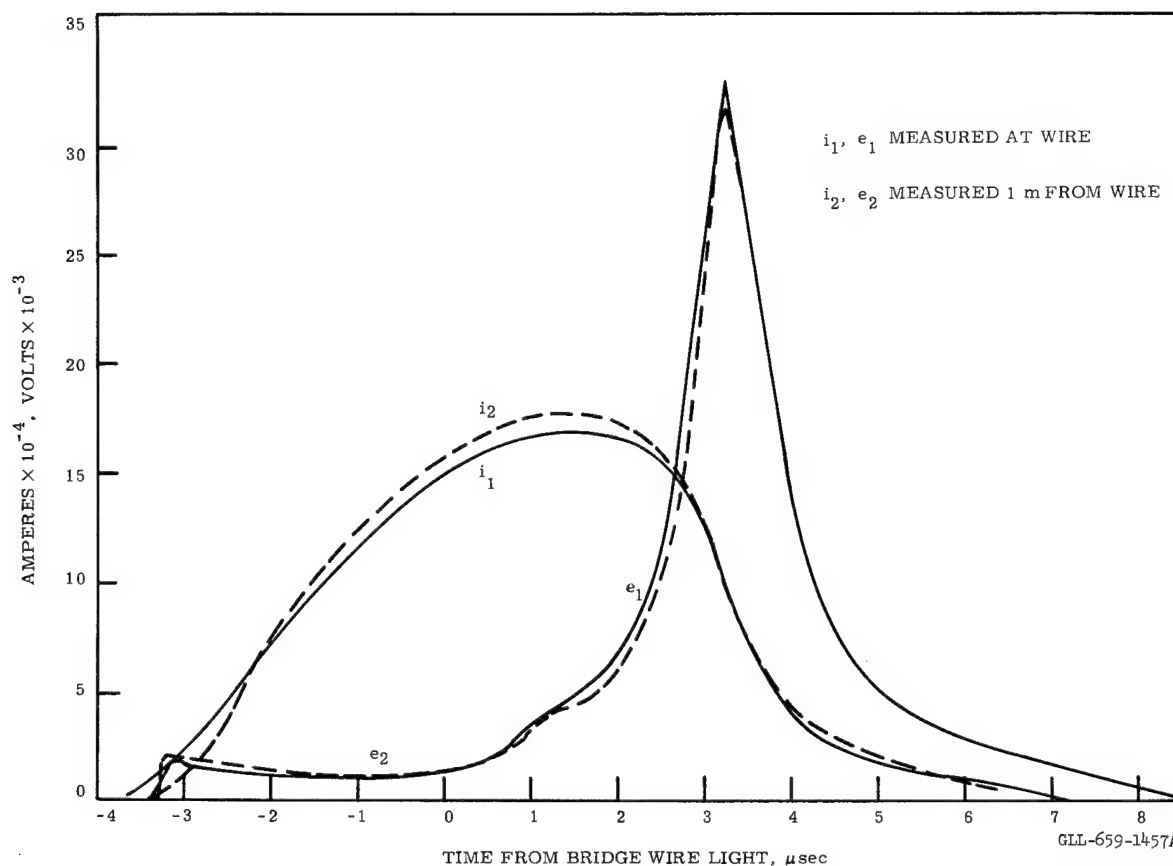

Fig. 7. Current and voltage from each of two measurement stations after explosion in air with bank charge voltage of 17.9 kV (Shot 47).

Component Calibration

Resistance of the Park-type shunt was checked with a Kelvin bridge. Integrated pickup-loop signals were calibrated dynamically for current using formula 7 of Ref. 2.

All low-voltage attenuator combinations introduced for either voltage or current signals were calibrated by using a well-regulated 10-V dc supply and four-digit voltmeters accurate to ± one digit to monitor input and output. A similar method was used to calibrate the vertical deflection sensitivity of the oscilloscopes. The calibration procedure for the high-voltage resistive dividers is described in the appendix.

Noise Reduction

Oscilloscopes which permit signals to be applied directly to the CRT plates were used because they are much freer from noise induction than amplifier-driven oscilloscopes. The latter require screen room and power line filters to reduce stray field noise effects of the bank discharge.

Possible Improvements

Future improvements could include a more expedient method to carry out the energy integration process by means of an electronic integrator circuit fed directly with the current and voltage signals during an explosion. A similar concept could be used to display the dynamic resistance of the wire by electronically taking the quotient of the voltage and current signal during an explosion. Such improvements would yield all pertinent records of the wire explosion history immediately at the time of the explosion.

OPTICAL TECHNIQUES

In order to check the energy measurement technique by a nonelectronic method, the velocity of the shock wave in air produced by the exploding wire was measured. This velocity is a function of shock pressure which is related to wire energy. In actual use the shots would be fired in water or a solid; however, only gas provides a large enough variation of shock speed with pressure to be useful. The tank mentioned in the section entitled "The Circuit" was fitted with windows at the ends and a pipe with a key way along the top. This pipe served as an optical bench for mounting a flash lamp (with iris diaphragm) and a Fresnel condensing lens and aligning them with the camera axis. Provision was also made for mounting a scale on the bench to permit precise determination of magnification. The whole could be shifted in space so that its axis passed through the wire.

A Beckman-Whitley Model 200 framing and streaking camera was used. The Fresnel lens was focused in such a manner that a reasonable approximation to a schlieren system was obtained. Resolution was at least 0.1 mm at the wire, according to photographs of a scale.

A small exploding wire was synchronized with the main wire, and the time between its first light output and the fiducial mark on the oscilloscope traces determined by a photocell. This wire was included in all pictures, and thus provided time reference throughout.

Figures 8 and 9 show framing and streaking camera pictures from wires exploded at bank charge voltages of 15.3, 17.9, and 20.6 kV in air. Interframe time is shown. The fine line on the framing records is the blank caused by the slit of the streak part of the camera.

DATA ANALYSIS

The oscilloscope traces were read on a digitized microscope. These data, together with calibration curves for the oscilloscopes and the high-voltage divider, various attenuation constants, and time calibrations were put into a program for an IBM 7094 computer.

The program then computed i(t), e(t), $\int_0^\infty ei\,dt$, $\int_0^\infty i^2 R_{external}\,dt$, and $R(t) = e/i$. These results were printed and plotted for use.

The streaking camera records, which were on 35-mm film, were also read on the digitized microscope, and the data fed into another program. This computed X(t), where X is the distance from the center of the wire to the shock wave, and $(2X)^2$ vs t, and plotted both. Since two values of X vs t occur in each experiment, the code also produced a mean value. The timing on the streaking camera record was linked to that on the oscilloscope records through the bridge wire and fiducial time mark mentioned above. Differences in absolute times among experiments were apparently due to jitter in the ignitron switches.

RESULTS

A total of 24 experiments, at various energies, were performed to test this technique. Table I presents measured energy and various other parameters vs bank energy for each shot. Figures 10(a), (b), and (c) show plots of e(t), i(t), E(t), and R(t) for the experiments whose oscilloscope traces are shown in Fig. 3 and whose streaking and framing camera records are shown in Figs. 8 and 9.

Figure 11 is a plot of $(2X)^2$ vs t from the streaking camera records for those experiments. Bennett[7] used Lin's similarity solution[8] to relate the square of the slope of this curve when it becomes a straight line to the energy per centimeter of the wire. It is believed that at best only Bennett's first-order solution is useful here; namely, $E = 7.24\,m^2$ where m is the slope of $(2X)^2$ vs t, and E the energy per centimeter after subtracting the vaporization energy (2.97 kJ for 7.5 cm). Figure 12 shows m^2 vs E

[7] F. D. Bennett, Phys. Fluids 1, 347 (1958).

[8] Shao-Chi Lin, J. Appl. Phys. 25, 54 (1954).

Streak
line →

Bridge
wire →

1.75 μsec
per frame

Shot 40
15.3 kV

1.75 μsec
per frame

Shot 47
17.9 kV

1.25 μsec
per frame

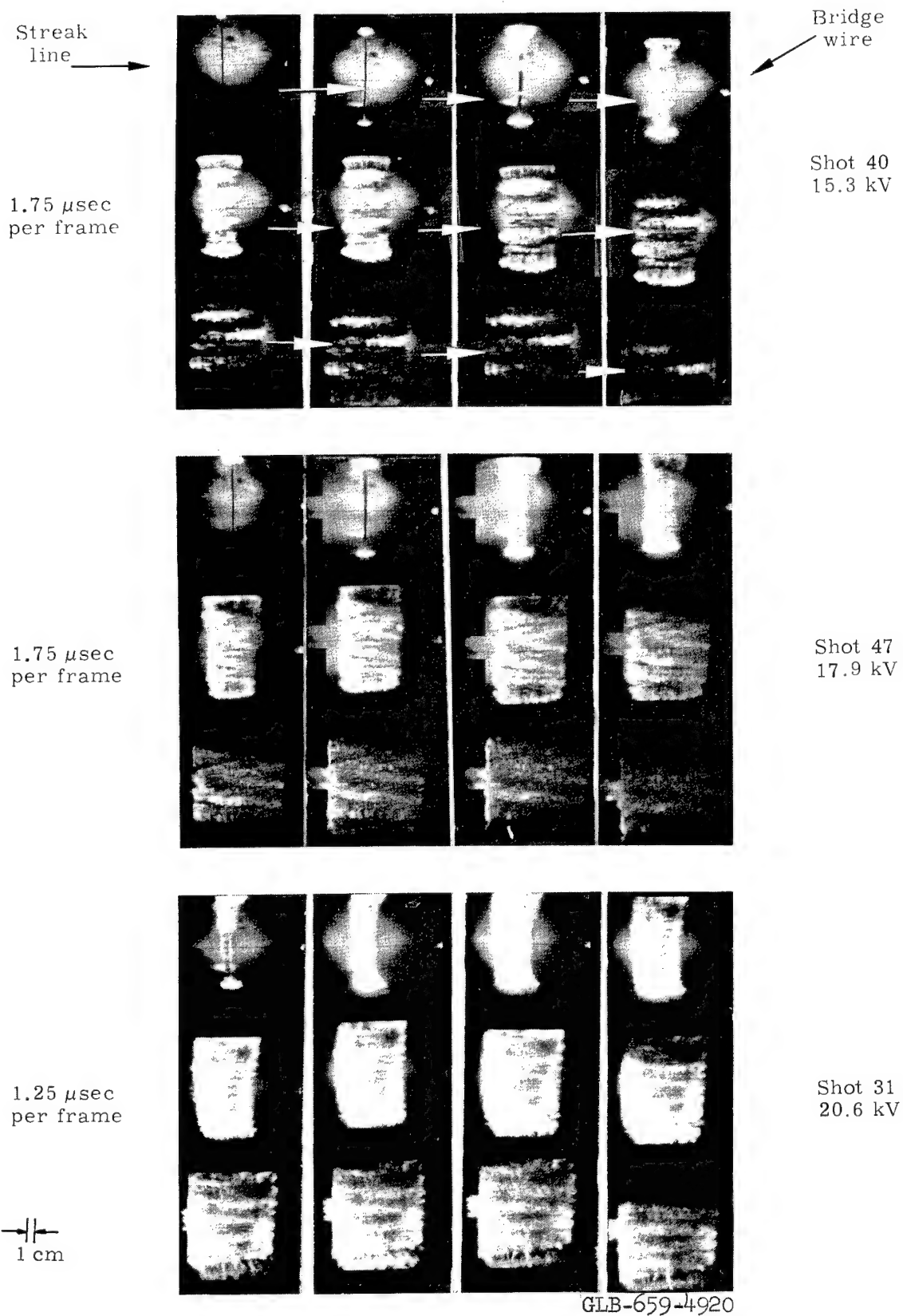Shot 31
20.6 kV

⊢|⊣
1 cm

GLB-659-4920

Fig. 8. Framing camera records from three shots in air with various
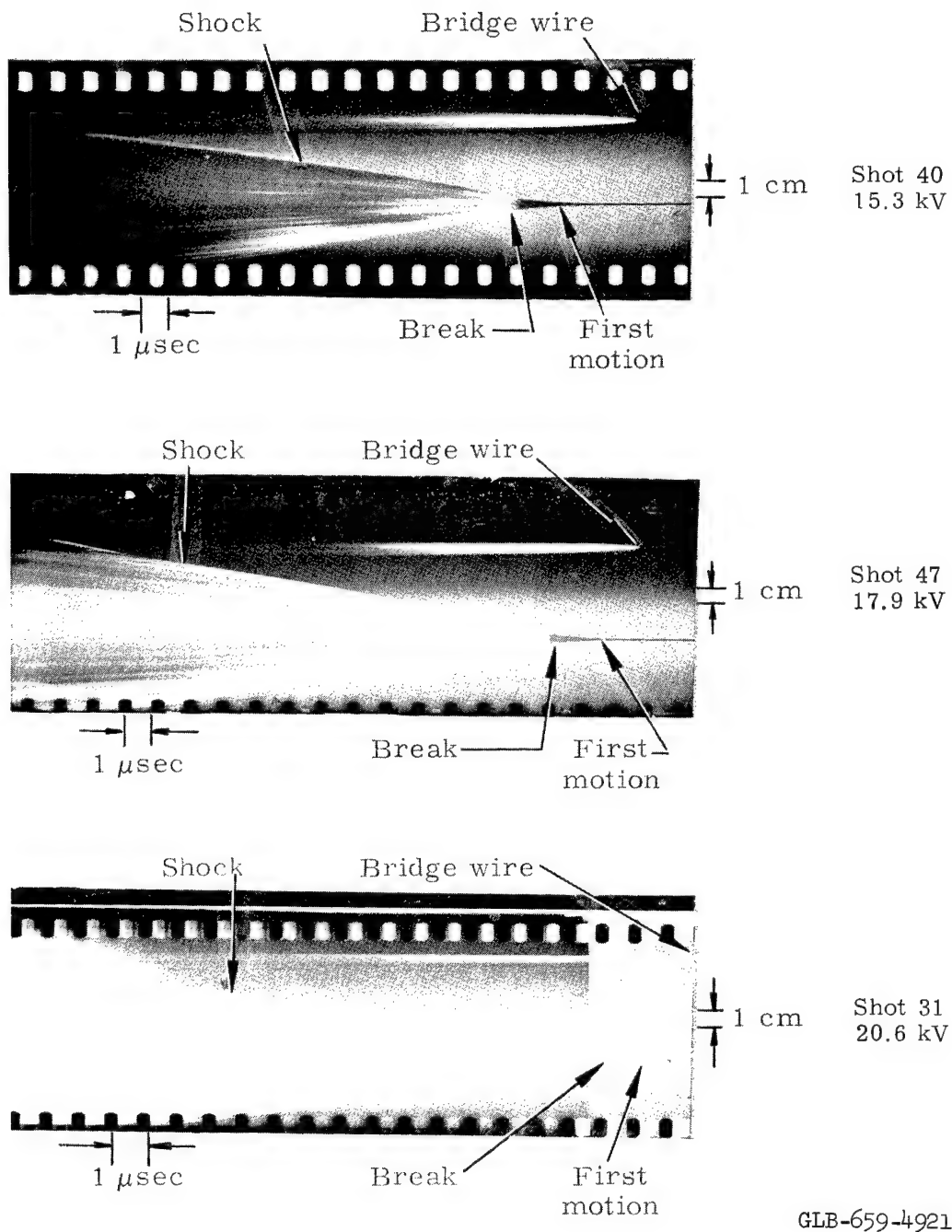bank charge voltages.   Time progression is indicated on upper picture.

Fig. 9. Streak records from three shots in air with various bank charge voltages. Time progresses from right to left.

Table I. Measured energy and other parameters vs bank energy for each shot (voltage in kV; energy in J; time in μsec from bridge wire).

Shot No.	Bank voltage	Capacitance	Bank energy	Wire energy	2nd meas. energy	$E-E_{vap}$ cm	Slope of $(2X)^2$ vs t	$(Slope)^2$	Time of energy "knuckle" ±0.2	Time of streak "break" ±0.2
17	17.9	41.8	6696	3412		65	3.03	9.18	4.8	4.7
18	17.9	41.8	6696	3773		103	3.76	14.14	4.8	5.3
39	15.3	57.4	6736	4002		133	5.60	31.36	4.1	4.6
40	15.3	57.4	6736	4230		164	5.31	28.20	4.3	4.4
45	15.3	57.4	6736	4130	3851	151	5.19	26.93	5.0	5.0
46	15.3	57.4	6736	4019	3777	136	5.05	25.5	5.4	5.2
13	20.6	41.8	8870	5394		314	6.21	38.56	3.7	3.5
14	20.6	41.8	8870	5218		296	5.56	30.91	4.6	4.5
15	20.6	41.8	8870	5503		334	6.87	47.19	3.3	3.0
10	17.9	57.4	9195	5748		366	5.64	31.80	4.5	4.3
33	17.9	57.4	9195	5587		345	6.19	38.32	3.4	2.9
34	17.9	57.4	9195	5452		327	6.38	40.70	3.3	3.2
35	17.9	57.4	9195	5887		385	6.85	46.92	3.4	3.2
38	17.9	57.4	9195	5831		377	6.94	48.16	3.1	2.8
43	17.9	57.4	9195	6313	6080	441	7.09	50.26	3.8	3.7
44	17.9	57.4	9195	6047	6368	406	6.93	48.02	4.2	3.8
47	17.9	57.4	9195	5809	5596	374	7.39	54.61	3.5	3.4
48	17.9	57.4	9195	6004	5833	400	6.97	48.58	3.5	3.4
19	24.1	41.8	12138	7987		664	- -	- -	2.7	2.5
26	20.6	57.4	12180	9235		831	- -	- -	2.7	2.3
27	20.6	57.4	12180	8628		750	- -	- -	2.3	1.8
28	20.6	57.4	12180	8649		753	10.16	100.0	2.2	2.1
30	20.6	57.4	12180	8419		722	8.98	80.64	2.6	2.6
31	20.6	57.4	12180	8433		724	9.38	87.98	2.5	2.5
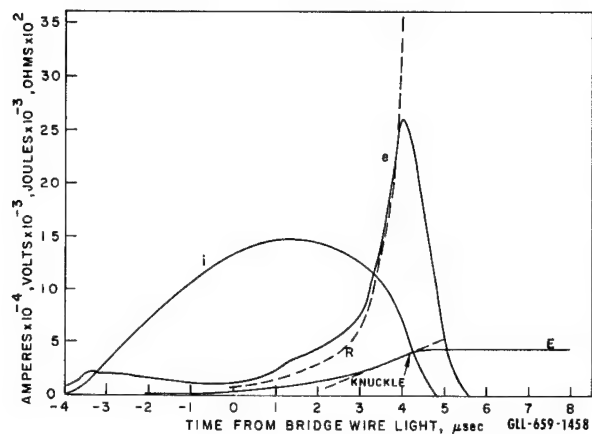
(a) Shot 40 (15.3 kV)
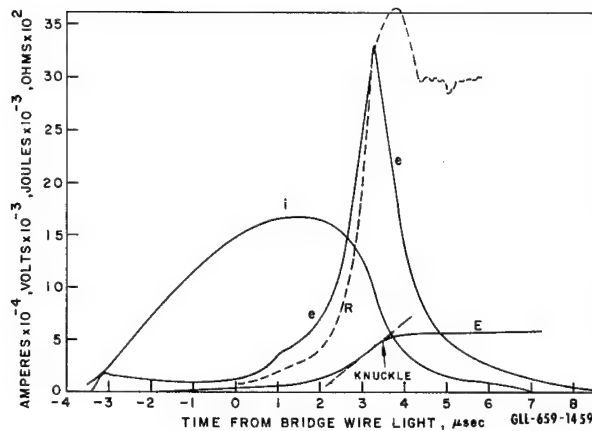
(b) Shot 47 (17.9 kV)
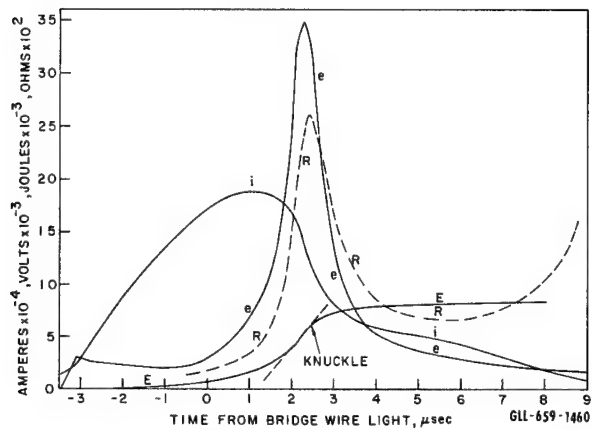
(c) Shot 31 (20.6 kV)

Fig. 10. Current, voltage, energy, and resistance for three shots in air at various bank charge voltages.
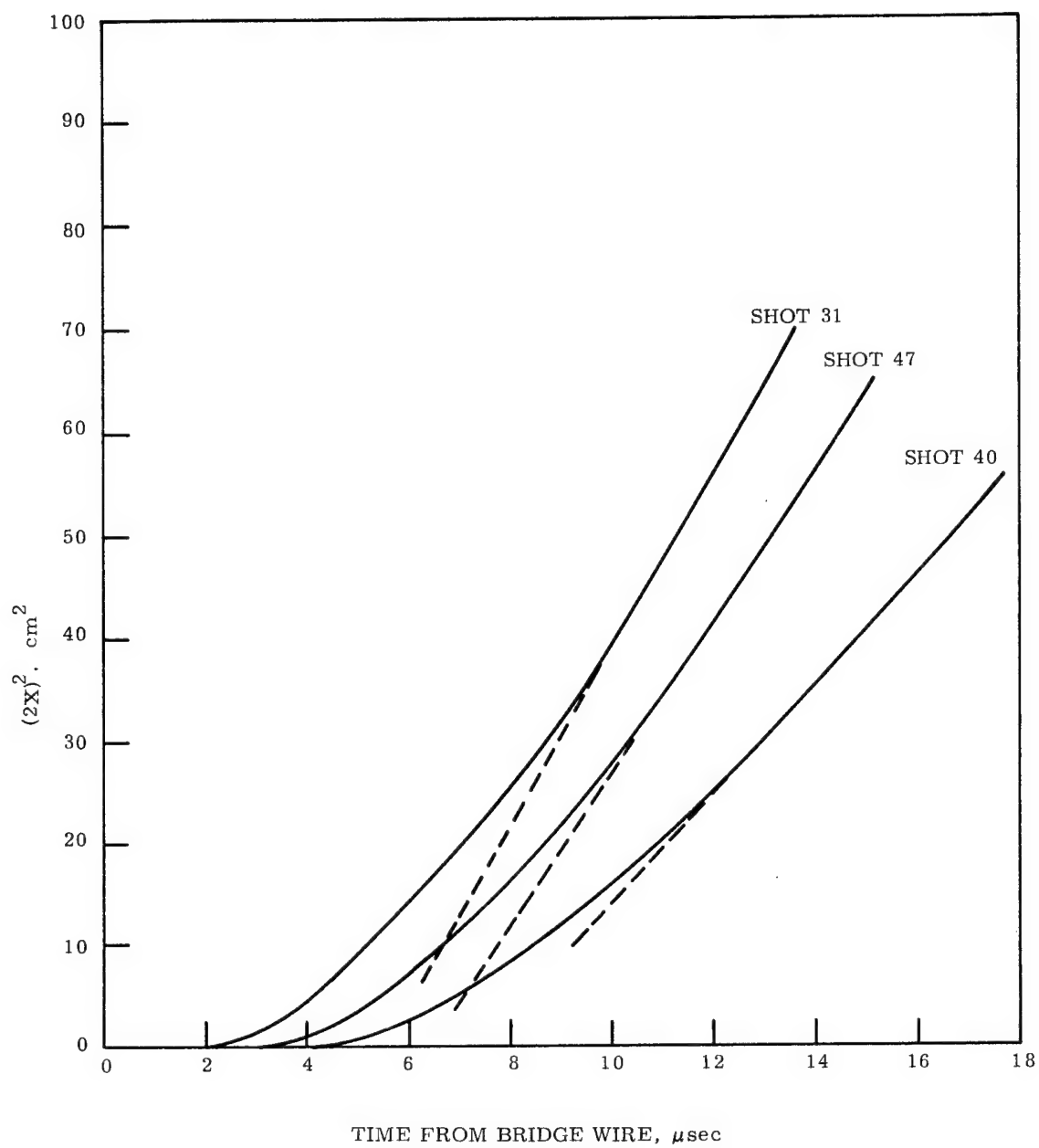
Fig. 11. Square of shock wave diameter vs time for Shots 31, 47, and 40 (taken from streaking camera records).
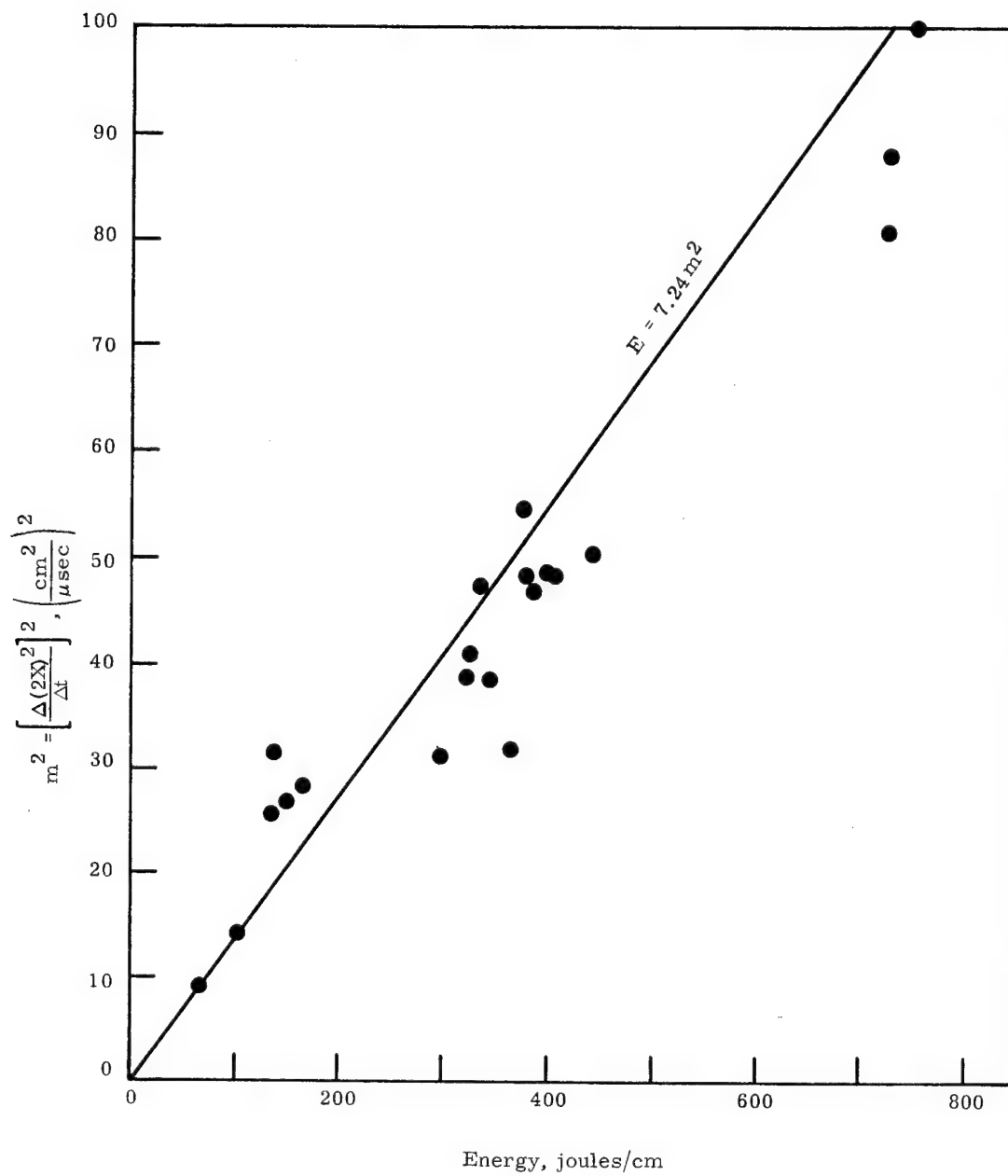
Fig. 12. Square of the slope of shock wave diameter squared vs time curve vs energy for 19 experiments.

for all experiments whose streaking camera records were long enough to observe the maximum slope. The scatter (also observed by Bennett et al.[9]) can be understood by close observation of the framing pictures. It should be noted that the edges of the shock front are rather ragged. Thus, the measured speed depends on precisely where on the wire the streak slit is aimed. Furthermore, in Fig. 12, the measured slopes of X vs t have been raised to the fourth power. The RMS deviation from Bennett's line is 23.5%. It should be noted that more than half of the points are below the line. Initial conditions might not be quite the same as his, though there was no evidence of this. Actually, of course even first-order theory probably does not hold at these energies.

The streaking camera records (Fig. 9) show that the wire first expands slowly followed by a sharp break in the slope of the expansion, and the shock wave appears. When this streaking camera record is correlated with the electronic energy measurement, two interesting things are observed: (1) the energy necessary to vaporize the wire is deposited quite early in the slow expansion, and (2) the break in slope in the streaking camera record generally corresponds well with the "knuckle" at the top of the energy vs time curve. Thus, the rapid expansion of the wire occurs at the end of the rapid energy input. That this phenomenon has not been observed before, to the knowledge of the authors, is probably due more to the speed of others' capacitor banks than the resolution of their cameras.

In order to test maximum wire energy acceptance of the system, wires were exploded at 22 kV in air and in water. Figure 13 shows the result (see traces in Fig. 6). In air, the wire eventually accepted 8736 J; in water, presumably because of greater confinement, 9555 J.

When $\int_0^\infty ei\,dt$, $\int_0^\infty i^2 R_{external}\,dt$, and the energy remaining on the bank are summed, 90% of the bank charge energy is accounted for if the initial external resistance of $0.015\,\Omega$ is used. If a larger value of resistance is assumed, to allow for the observed increase with time (see section entitled, "The Circuit"), a greater fraction of the energy is obtained.

CONCLUSIONS

Considering the inherent inaccuracy of shock wave measurements, Fig. 13 tends strongly to confirm the electronic energy measurements. The correlation between the "break" in the streaking camera record and the "knuckle" in the energy curve also tends to confirm the electronic energy measurements, since it is reasonable to believe that the sudden rapid expansion of the wire is the cause for the cessation of energy-acceptance by the wire. Finally, the ratio of wire energy to bank energy is similar to that observed by Bennett et al.[9] at much lower energies.

It is therefore concluded that the electronic technique described here can measure the energy deposited in an exploding wire to within at least 25%. The accuracy is probably

[9]F. D. Bennett, H. S. Burden, and D. D. Shear, Phys. Fluids 5, 102 (1962).
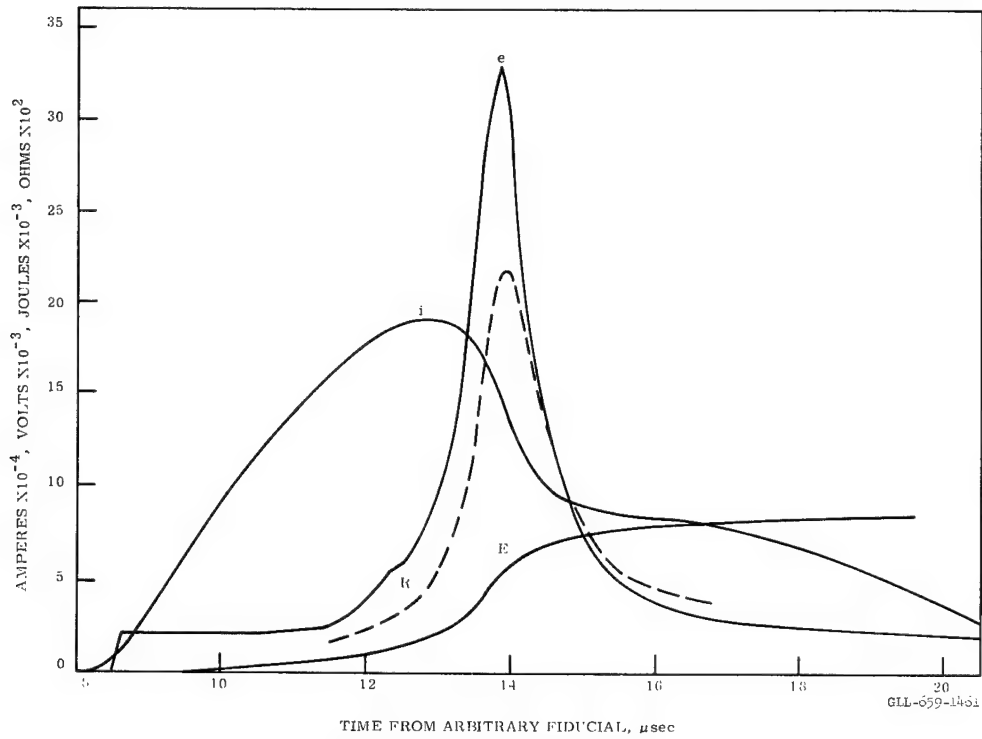
(a) Shot 54 (air)
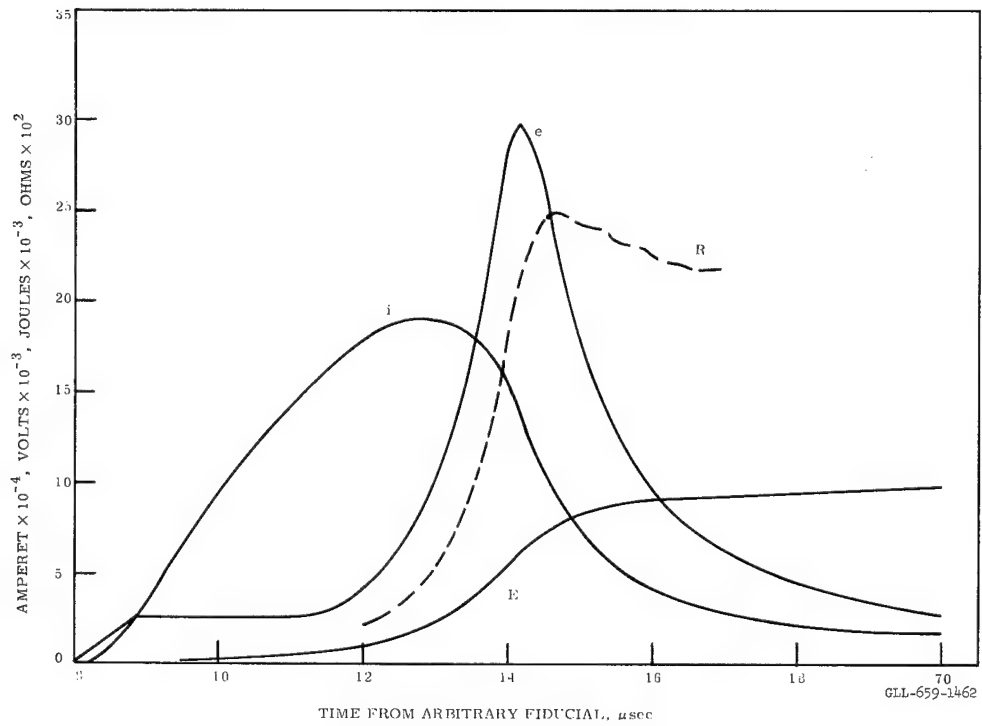
(b) Shot 53 (water)

Fig. 13. Current, voltage, energy, and resistance for wires exploded with bank charge voltage of 22 kV.

greater, and the scatter in wire energy vs bank energy shown in Table I is probably real; there is, however, no nonelectronic evidence to confirm such conclusions. As measured, the energy density per original cubic centimeter, even excluding vaporization energy, is an order of magnitude greater than that from high explosive. However, since the wire starts to expand in this case before all of the energy is deposited, energy density at the time of final energy input may be substantially lower. A faster source will correct this deficiency.

ACKNOWLEDGMENTS

APPENDIX

General Features of Exploding-Wire System Layout, Diagnostics, and Control

The capacitor bank room is shown in Fig. A1 with the Beckman-Whitley Model 200 simultaneous framing and streaking camera in the foreground, the water tank with windows and splash cover on the right, the capacitor bank cabinet in the center background, and a rack containing part of the camera control equipment, flash-lamp pulsers, and a bridge-wire pulser on the left. Figure A2 is an interior view of the capacitor bank cabinet.
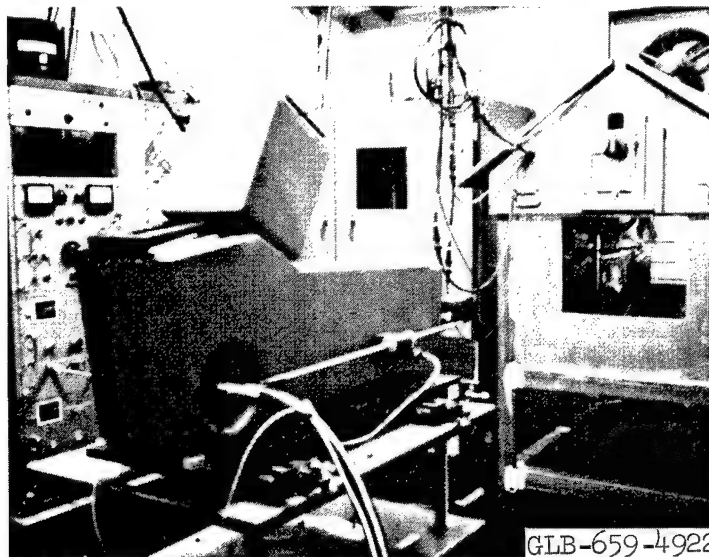

GLB-659-4922

Fig. A1. Test area.

The control and instrumentation room is shown in Fig. A3. A voltage measurement oscilloscope, a current measurement oscilloscope, and an oscilloscope to check for restrikes are shown at the left. Not shown are two additional voltage and current measurement oscilloscopes. Three control racks are shown in the center of the picture. The two on the left hold a camera control chassis, power supplies for flash-lamp and bridge-wire pulsers, fiducial-mark and time-mark generators and amplifiers with associated switching panels, a time-delay generator, a time-interval meter, and associated selector panels. The third control rack holds a chassis to supply the bank ignitron firing pulse and to control bank charge and crowbar vacuum switches, a bank voltage-indicating meter chassis, and an oscilloscope camera-shutter-control chassis. The cabinet on the far right is a 20 kV, 100 mA dc power supply for bank charging.

The control scheme allowed either automatic firing of the bank by the high-speed camera, or manual control firing. The sequence of events in the total wire-explosion process could be altered by use of the delay generator which provided six separate delay channels. The time interval between any two selected events could be measured
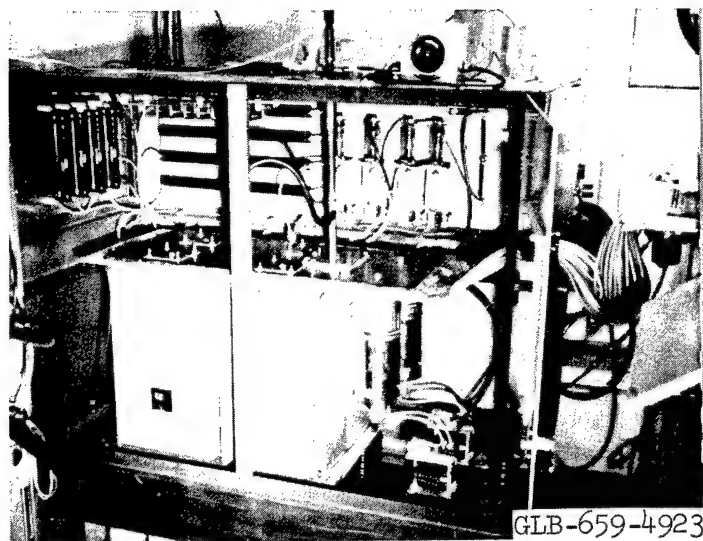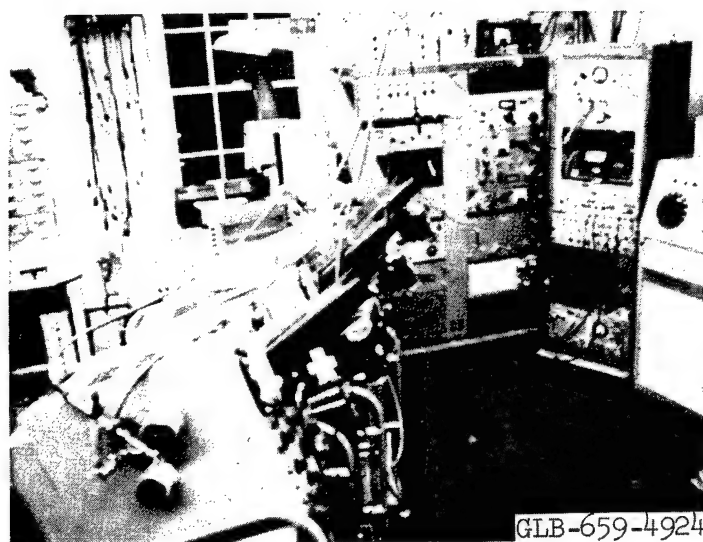
Fig. A2. Capacitor bank.

Fig. A3. Control and instrumentation room.

by the time interval meter. A dry-run pulser to simulate the camera fire pulse could be used to check out the system.

Electrical safety features included automatic bank crowbar interlocks on the bank room doors and on the bank cabinet doors. A manual crowbar could be tripped from a distance. Red lights flashed and a bell rang when the manual crowbar was lifted.

Transmission Line Construction Details

The Park-type current shunt was built into the bottom side of the flat-plate line near the wire location by arranging an overlapping insulated break in the bottom line. The shunt was electrically connected between these overlapping sections, the shunt housing flange being bolted to the lowermost section. The shunt insulator and center stud projected through a hole in this section. The threaded center stud continued on to project through a hole in the uppermost section. The stud was connected to this section by means of a nut threaded on the stud and bearing on the plate. The shunt housing projected down through a hole in the support plate. A hole was also cut in the top plate of the transmission line to allow the center stud of the shunt to project up through it. A capped cylinder welded around this hole was filled with oil to insulate the stud from the top high-voltage plate. Used between the plates were O-ring seals to prevent oil leaks, and the plates were compressed together by means of "outrigger" micarta clamps.

Shown in Fig. A4 is the flat-plate transmission line assembly before installation in the water tank. The input end of the line is at the upper left. The portion of the line projecting toward the viewer includes the Park-type current shunt hanging down from the bottom plate through a hole in the ground support plate. Its output signal cable passes through a hole in one of the main micarta clamps. The jaws to clamp the wire holders appear at the output end of the line. The metal "outrigger" bars fit in runners on the tank wall and could be clamped to make metallic contact with the tank wall at any point over a 10-in. vertical height range.

In Fig. A5 the top high-voltage plate is viewed from above, the camera looking down into the oil reservoir which insulated the current shunt stud projecting up into it.

Two views of the transmission line installed in the water tank are presented in Fig. A6. Figure A7 shows two views of the line with the lower voltage divider and compensating pickup loop installed.

Figure A8 shows a voltage divider and compensating pickup loop installed at the top of the line.

Mixing Data Signals with Time-Marker System Signals

The mixing of the voltage divider, the compensating pickup loop, and the time-marker system signals to feed a 517A oscilloscope is illustrated in Fig. A9. Figure A10 illustrates how a current signal derived by integration of a pickup loop signal is
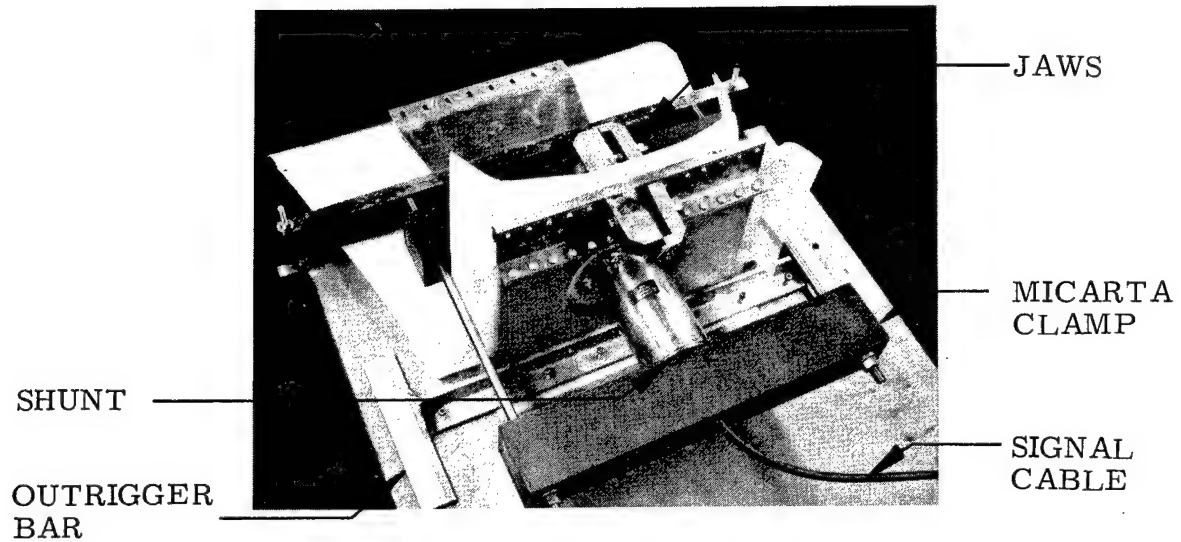
JAWS

MICARTA
CLAMP

SHUNT

SIGNAL
CABLE

OUTRIGGER
BAR

Fig. A4. Flat plate transmission line assembly.

SHUNT
STUD

OIL

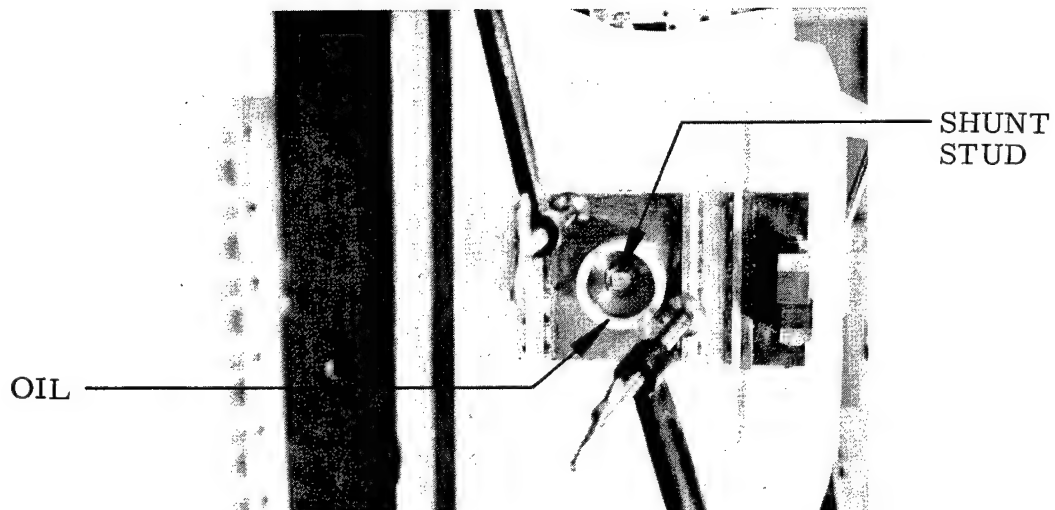Fig. A5. Oil reservoir for insulating the shunt stud.

FLAT PLATE TRANSMISSION LINE

CABLES
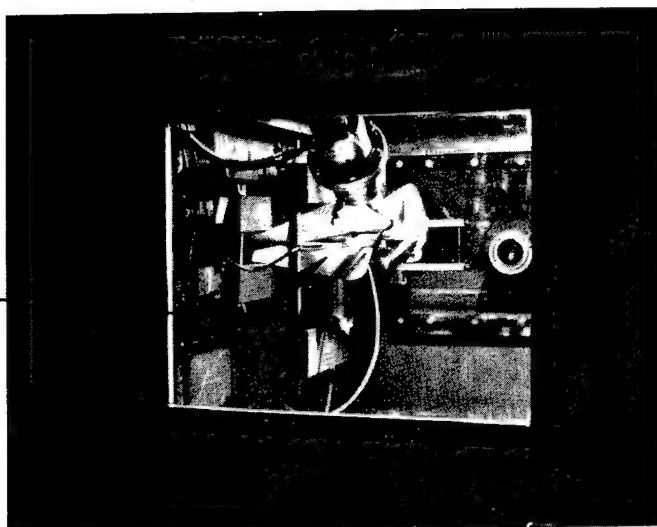FROM
CAPACITOR
BANK

(a)

OIL
RESERVOIR
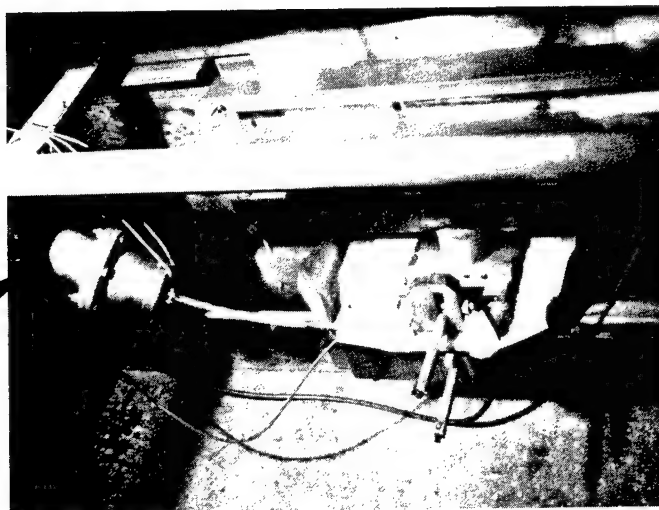
WIRE HOLDER
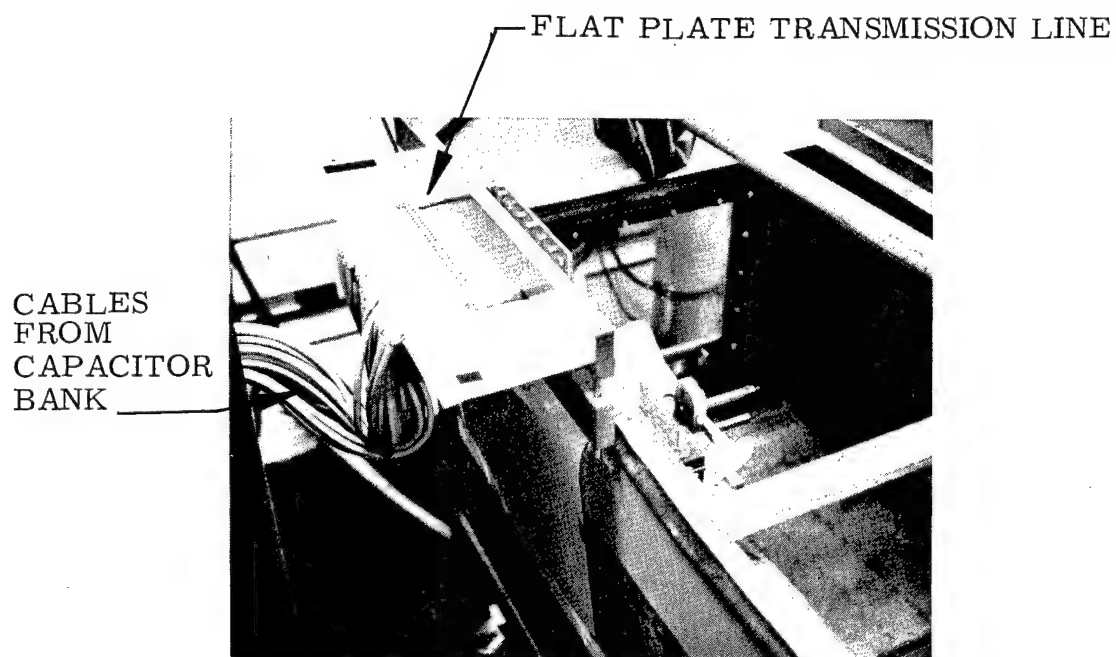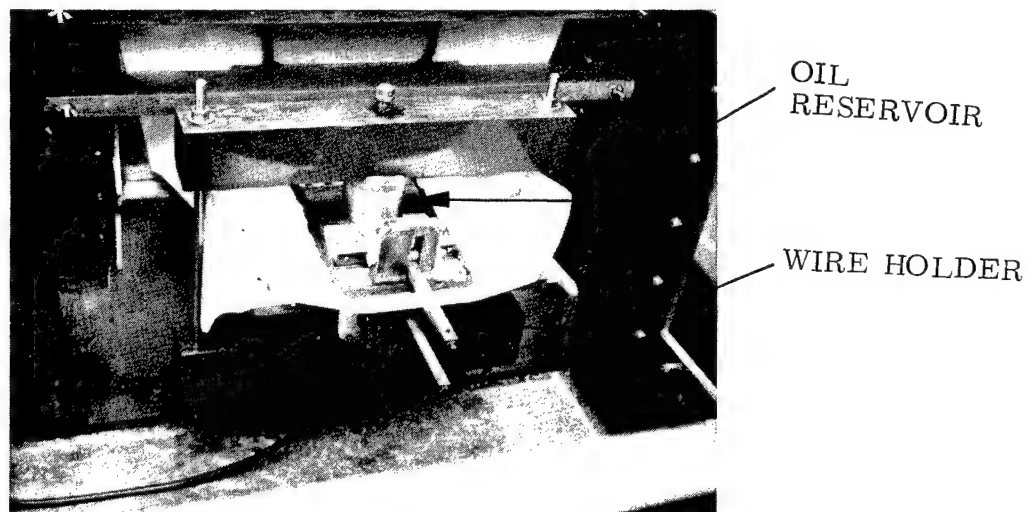
(b)

Fig. A6.   Transmission line in water tank.

PICKUP
LOOP

(a)

LOWER
DIVIDER

(b)

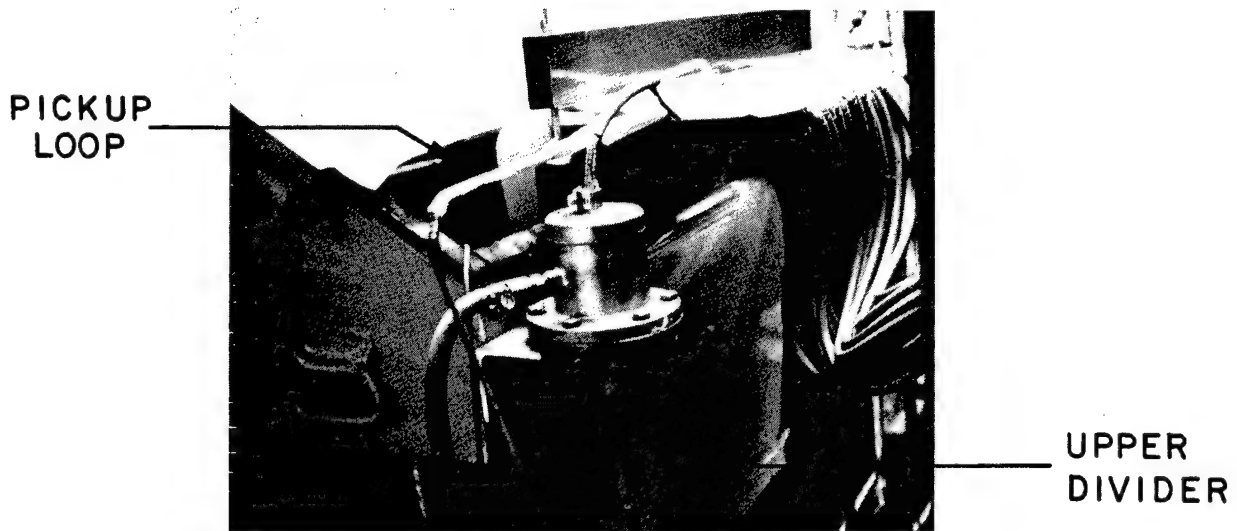Fig. A7. Voltage divider and pickup loop near wire.

Fig. A8. Upper voltage divider and pickup loop.

mixed with the time-marker system signal to feed an oscilloscope. The mixing of the Park-type current shunt signal with the time-marker system signal to feed an oscilloscope is illustrated in Fig. A11.

The mismatched time-mark system with fanout did not present a problem because one could easily ascertain the incident timing wave even though its trailing edge showed minor reflection steps. However, it was necessary that the timing signals be of an amplitude high enough to overcome the marker signal reduction due to mismatch and the attenuation introduced by the 560 Ω isolation resistor teed into the 50 Ω system. Again, for very fast systems using sweep speeds considerably faster than those used in this case, such a mismatched time-mark system cannot be used. Tektronix 507 Mod. 226EL oscilloscopes with separate direct access to each vertical deflection plate will permit an impedance-matched, time-mark system fed in series through several oscilloscopes on one of the plates while data signals can be applied individually to the other plates. The state of the art here, however, limits repetition rates to approximately 10 Mc for pulses of sufficient amplitude to display on a 507 Mod. 226EL. If shorter timing intervals are required, one must resort to either mixing sine wave timing signals with the data signal or displaying the timing sine wave separately.

Design Principles and Construction Features of the Pickup Loops

The pickup loop used in the voltage measurement scheme is arranged to meet the requirement for appearing as 50 Ω when viewed from its signal transmission cable by placing a 50 Ω resistor in series with the loop. The inductance of the loop was held to such a value that the resultant L/R time of the combination did not exceed 2.5 nsec, or a related step-function risetime response of about 7 nsec.

A five-turn pickup loop is shown in closeup and in complete assembly in Fig. A12. The loop and series resistor were attached across the end of a few feet of RG-213/U
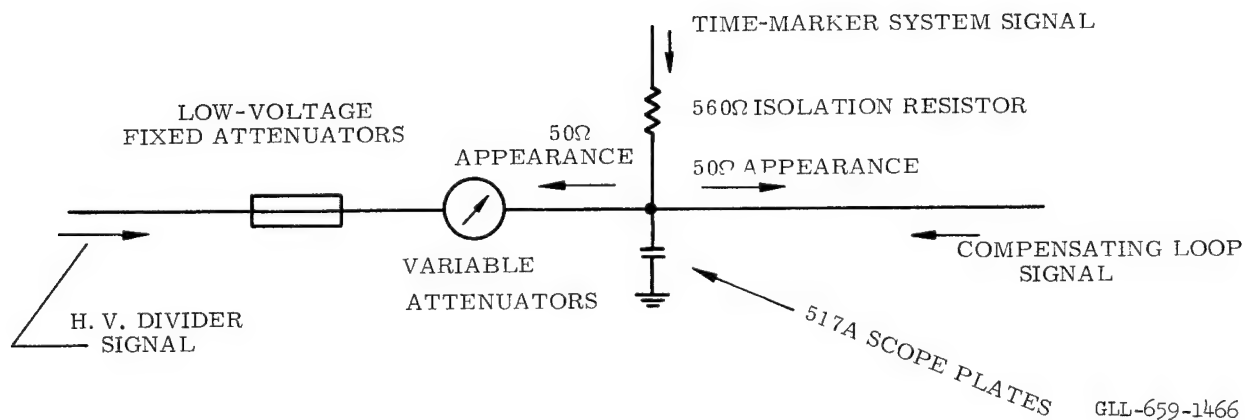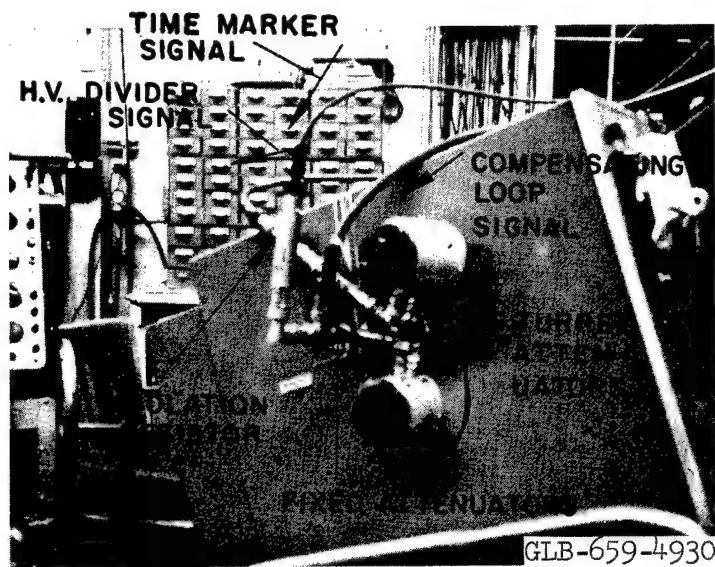
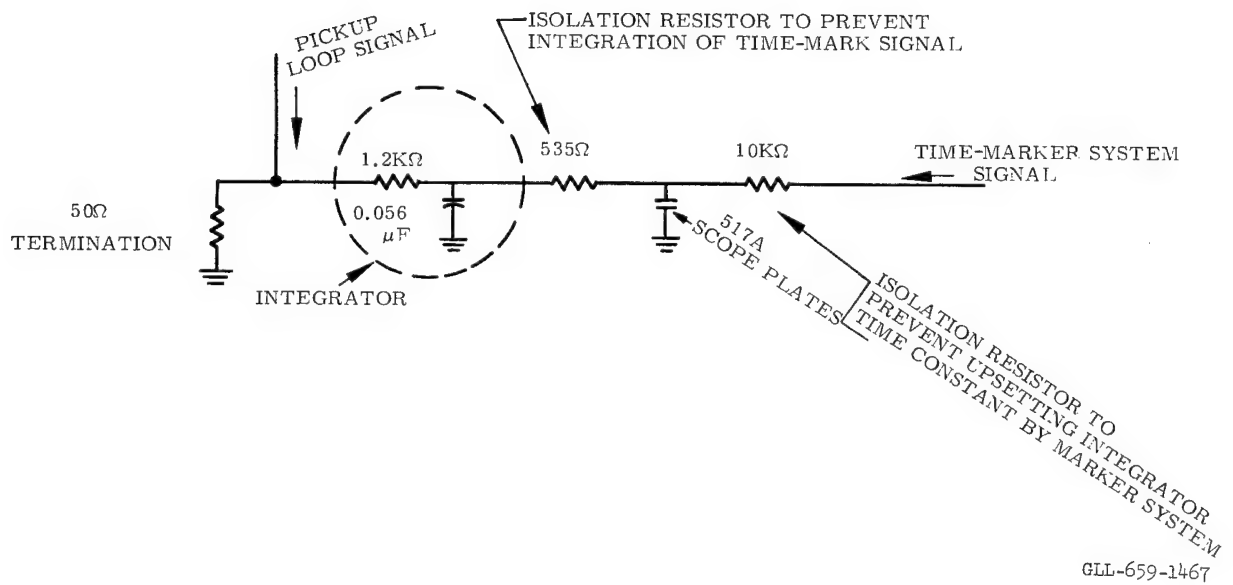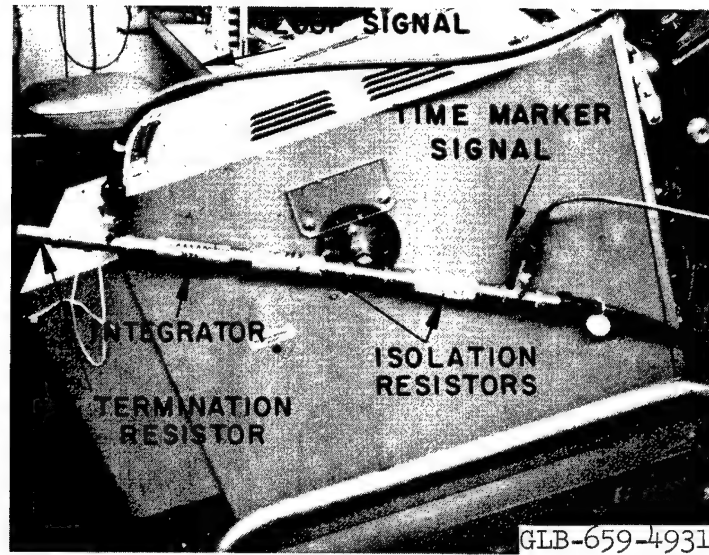Fig. A9. Mixing of voltage and time-mark signals. (Photo above, diagram below.)

Fig. A10. Mixing of current (derived from pickup loop) and time-mark signals. (Photo above, diagram below.)
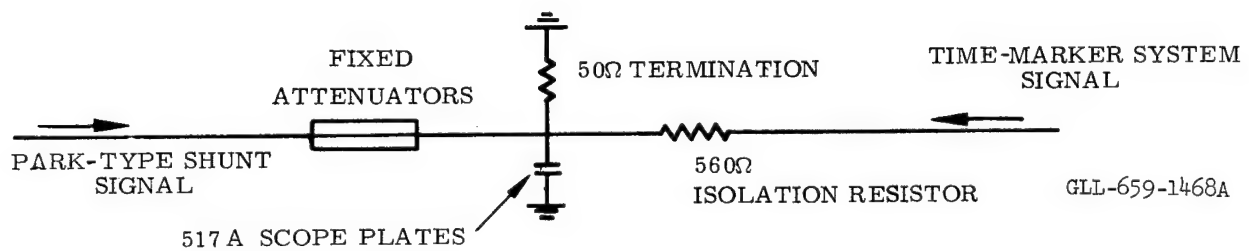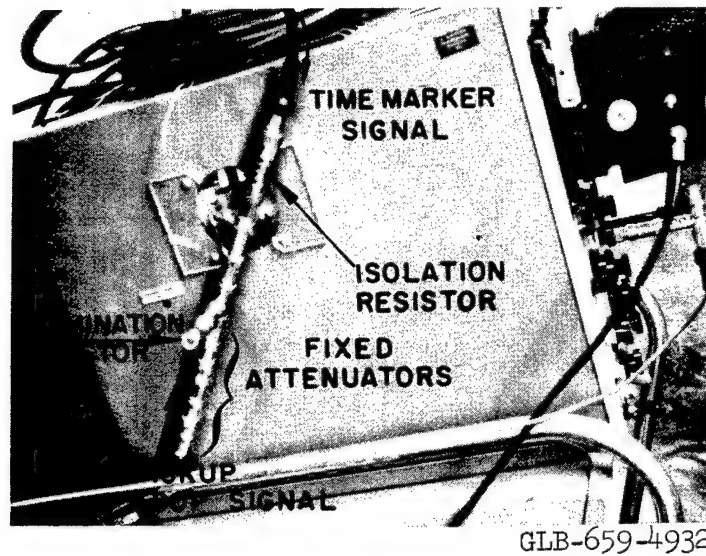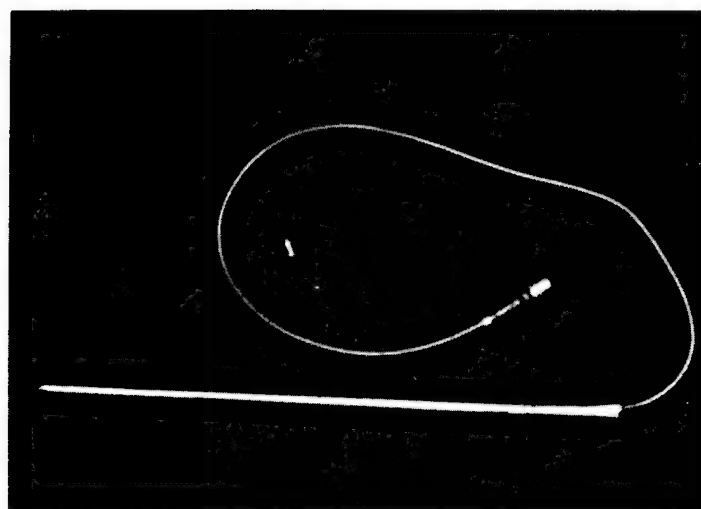
GLB-659-4932

Fig. A11. Mixing of current (sensed by Park shunt) and time mark signals. (Photo above, diagram below.)

(a)

(b)　　　GLB-659-4933

Fig. A12. Pickup loop: (a) closeup, (b) complete assembly.

cable. The cable was inserted within a close-fitting brass tube about 2 ft in length and kept insulated from the tube until the cable braid was soldered to the end of the brass tube at the loop location. The brass tube portion was wrapped with about 10 turns of 2-mil mylar sheet before being inserted in a transverse slot on the inner surface of the grounded transmission plate. The interline sheet mylar was the primary insulation for isolation of the loop.

The assembly procedure was as follows. The cable was first inserted through the brass tube. A lucite coil form of about 5/32-in. outside diameter and 1-in. length was drilled through its center to accept the center conductor of the cable and the resistor lead. The coil form was turned down at one end for a distance of 1/4 in. to match the diameter of the polyethylene cable insulation and counterbored to a diameter of 3/32 in. at the opposite end to a depth of 1/4 in. A 50 Ω 1/4 W composition carbon resistor was inserted into the counterbore; its inner lead was soldered to the cable center conductor which extended into the lucite form. This solder connection was effected by access through a small radial hole in the form and made so that the lucite form abutted the end of the cable polyethylene insulation. This juncture was covered with a wrap of mylar tape.

A previously turned-back portion of cable braid was then brought forward over the lucite form and the whole arrangement pulled back into the brass tube just far enough to leave about 1/2 in. of the lucite form projecting beyond the end of the tube. The braid was then cut off flush and soldered to the end of the tube. Copper wire of No. 20 gauge was wound evenly in five turns over the protruding portion of the lucite form and the wire end soldered to the end of the 1/4 W resistor which just protruded from the counterbore. This procedure was used regardless of the number of turns.

Most of the voltage measurements were made with 10-turn pickup loops because the sensitivity of the null adjustment is increased for higher magnitude loop signals. The risetime response of the pickup becomes worse, of course, as turns are added, but even a 10-turn pickup loop of this diameter is considerably faster than required for this particular capacitor bank. However in the case of extremely fast risetimes for imped-ance-matched, traveling-wave, exploding-wire sources, the risetime of such a pickup can be improved for a given coil inductance by placing a resistor across the end of the loop-signal transmission cable and shunting this resistor with a resistor-and-loop series combination. The values of these two resistors are chosen such that they present a resultant 50 Ω termination when looking from the signal cable into this loop arrangement. The resistor in series with the loop can be chosen high enough that for a given loop inductance it can reduce the signal risetime response of the loop arrangement to what-ever low value is required. This arrangement results, of course, in divider action, which if high enough can reduce the loop signal below permissible levels. However, the higher $d\phi/dt$ of faster systems helps to offset this effect. Also, if fast amplifier-driven oscilloscopes, such as a Hewlett Packard 175 or Tektronix 585, can be used, lower signal levels could suffice.

The pickup loops used for current measurement were of larger diameter and, therefore, of somewhat slower response than those used in the voltage measurement scheme. The use of the larger diameter pickup loops was necessary to obtain a larger amplitude signal to drive integrators feeding direct to the plates of a 517A oscilloscope. Again, these pickup loops could be faster with lower signal levels for amplifier-driven oscilloscopes.

The brass tube in this case was used to shield the cable braid against magnetic field induction, in order to insure coupling only at the loop location. However, it may be a better construction from the standpoint of electrostatic shielding not to solder the cable braid to the tube, but rather to keep the loop and signal cable completely insulated from the tube while extending the tube out to enclose the loop structure. It is possible to allow the magnetic field for signal induction to enter the tube only at the loop location by slotting the tube just in the immediate region of the loop.

Design Principles and Calibration Procedure for the High-Voltage Resistive Dividers

It is a requirement of this particular energy measurement scheme that the high-voltage divider present an effective resistance equal to the characteristic impedance of the output-signal transmission cable when seen looking from the cable into the divider output; namely, 50 Ω in this case. This requirement determines the total permissible divider resistance for a given divider ratio. The total divider resistance, or related attenuation ratio, must be chosen high enough that the divider represents an insignificant load in parallel with the wire and experiences inappreciable change in the effective 50 Ω presented by the output arm as seen looking from the signal transmission cable during the change in exploding wire resistance. The wire resistance change during those wire explosions investigated normally covered a range from about 0.001 to 0.1 Ω. This means that during these particular wire explosions the effective impedance of the divider as seen looking from the transmission cable into the divider output is, for practical purposes, equal to the resistance of the output arm in parallel with the resistance of the high-voltage arm of the divider.

A minimum divider-input resistance of 100 Ω or more would satisfy the requirement for insignificant loading in this case. However, for a 50 Ω output arm, a minimum divider resistance in the range of 2500 Ω is required in order to maintain closely the 50 Ω appearance of the output arm, independent of wire resistance. It must also be kept in mind that the effective resistance of the output arm as seen looking into the transmission cable is equal to the resistance of the output arm in parallel with the cable impedance. In the case of a 50 Ω arm and a 50 Ω cable, the effective output resistance is 25 Ω. This would result in a 100-to-1 divider ratio for a total divider effective resistance of 2500 Ω.

High-voltage resistance dividers of 100-to-1, 200-to-1, and 10-to-1 ratios were constructed, all with 50 Ω resistance in the output arm (effectively, 25 Ω when feeding a 50 Ω cable). Inadvertently, the design was incorrect for the 10-to-1 divider, because in

this case the total divider resistance is 275 Ω, resulting in only 41 Ω resistance as seen looking into the output during this type of wire explosion. This condition was remedied by adding a series resistor immediately at the output connection in order to raise this effective impedance to 50 Ω. This series resistor also serves as an additional low-voltage attenuator.

A more direct approach for the 10-to-1 dividers would have been initially to have chosen some value above 50 Ω for the output arm, so that when it is effectively paralleled by the high-voltage arm during a wire explosion the resultant resistance looking into the output would equal 50 Ω. However, either this approach or the remedy actually used are satisfactory only when the wire explosion history does not involve a dark pause or extremely high wire resistance; otherwise, the divider appears as a value significantly higher than 50 Ω during a pause. If dark pauses must be dealt with, then a total divider resistance must be chosen which is high enough to maintain the appearance of the characteristic impedance of whatever signal transmission cable is used when looking into the output arm over an effective wire impedance range from practically zero to infinity.

In the case of a 50 Ω cable and a 50 Ω output arm, the minimum divider resistance, as previously mentioned, must be in the neighborhood of 2500 Ω in order to make the divider insensitive to changes in wire resistance. This requirement results in a 100-to-1 divider ratio. However, no dark pauses were involved in this investigation, and the peak explosion voltages did not exceed 30 kV. It was decided, therefore, to use a 10-to-1 high-voltage divider with additional series low-voltage attenuators because the percentage change in attenuation ratio due to the voltage coefficient effect of the resistors was considerably less for the 10-to-1 dividers than for the 100-to-1 or 200-to-1 dividers. However, if the integration process to obtain energy can be carried out on a computer, nonlinear dividers are not necessarily objectionable because a high-voltage pulse calibration of the divider can be input to the code.

Pulse calibration of the dividers was carried out to 30 kV using a high-voltage, reflection-type attenuator fed in parallel with the high-voltage divider to be calibrated. The reflection-type attenuator was used as a high-voltage pulse measurement standard to ascertain accurately the magnitude of the input pulse voltage. Such attenuators have too short a pulse-width response for connection to high energy sources with long duration discharges, such as capacitor banks. These attenuators are limited for true response by the double transit time of the transmission cable by which they are fed. However, this limitation did not present a problem in this case for calibration of the dividers. The reflection-type attenuator and resistive divider were each fed through separate 200-nsec lengths of cable which were fed in parallel at their sending end by a thyratron-switched pulser having a risetime of about 40 nsec. The true pulse-width response of both the reflection-type attenuator and the divider under this condition of feed was limited to twice the transit time of their input cables, or an equivalent of 400 nsec, due to their mismatch to the cable in each case. This width was more than ample to permit calibration.

Figures A13(a), A13(b) and A13(c) illustrate for 10-to-1 dividers the improvement in linearity effected by increasing the number of series high-voltage resistor sections. A comparison of Fig. A13(c) and A13(d) illustrates that linearity suffers for higher resistance dividers such as the 200-to-1 compared to the 10-to-1. The increase in undulations on the top of the wave as voltage increases as seen in Figs. A13(a), A13(b), A13(c), and A13(d), is due to increased inductive energy effects of the pulse source, and is not any "ringing" divider response.

The risetime response of all of the high-voltage dividers was measured on a sampling oscilloscope when fed with a 20-psec risetime pulser through a 22-nsec length of RG-213/U cable. The oscilloscope risetime response was 100 psec. Figure A14(a) shows a displayed risetime (10 to 90%) of 0.12 nsec for the pulser feeding the oscilloscope directly through the cable. Figure A14(b) shows a displayed risetime of 0.17 nsec for the same pulse after passing through the cable and a 10-to-1 high-voltage resistive divider. The calculated risetime response of the divider from these displays, assuming a gaussian response, is therefore 0.12 nsec.

Construction Features and Related Performance Characteristics of the High-Voltage Dividers

The high-voltage resistive dividers were composed of numerous 1/2 W composition carbon resistors built into an insertion structure of series cylindrical resistor sections and enclosed within a coaxial housing such that the geometrical characteristic impedance of the resistor cylinder within the housing represented 50 Ω. Figure A15 shows three typical resistive-divider inserts. Each cylindrical resistor section of each insert is composed of 24 resistors in parallel around the circumference. In each insert, the bottom section is the output arm of the divider and equal to 50 Ω. The remaining successive sections in series in each insert represent the high-voltage arm of the divider.

In Fig. A15, the insert on the left has a high-voltage arm of three sections, the middle insert has an arm of five sections, and the insert on the right, seven sections. For a given divider ratio, the risetime response to a 20-psec risetime pulse as displayed on a 100-psec risetime response sampling oscilloscope is somewhat better for the inserts with fewer sections. However, the percentage change in attenuation ratio up to a given input voltage due to resistor voltage coefficient is greater for those inserts with fewer sections because of a higher voltage stress per resistor section. It was determined that dividers composed of 1/2 W resistors which did not exceed about 1000 Ω per individual resistor and 5 kV pulse voltage per resistor section held the attenuation ratio shift during a pulse to a maximum of about 2%. The 10-to-1 dividers fell in this category, but the 100-to-1 and 200-to-1 dividers were more nonlinear due to considerably higher values of resistance for the individual resistors. All of the energy measurements in this investigation were made using 10-to-1 high-voltage dividers with seven sections in the high-voltage arm.
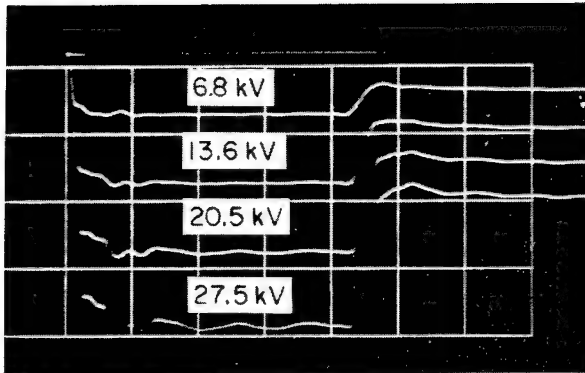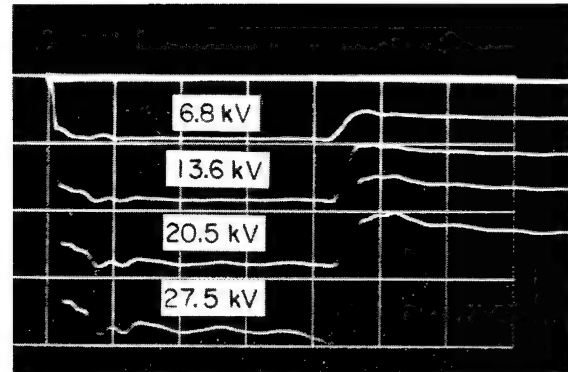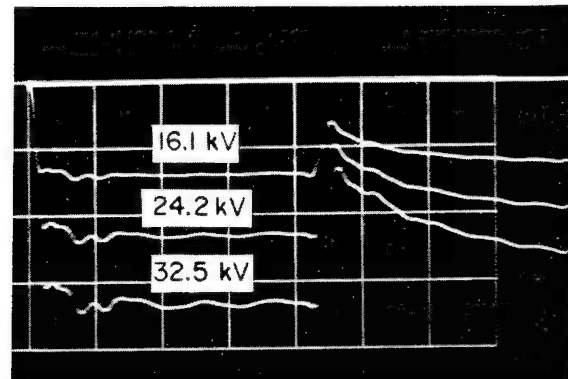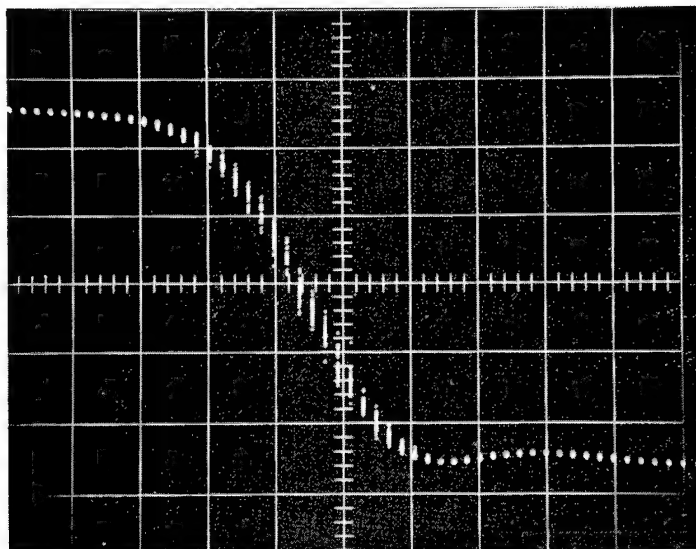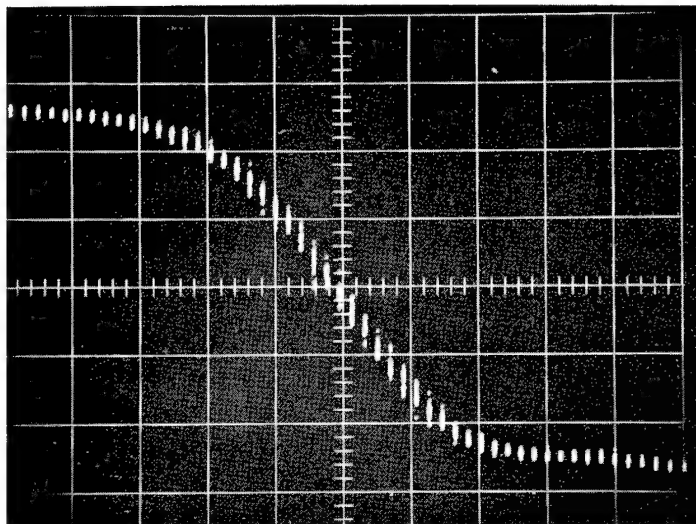
(a) (b)
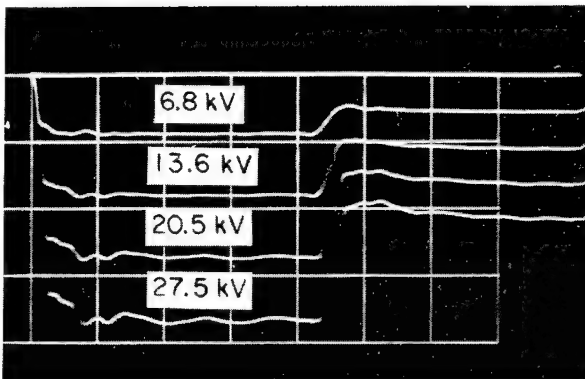
(c) (d) GLB-659-4934

Fig. A13. Calibration of high-voltage resistive divider. Horizontal, 100 nsec/division.

(a) 10:1 divider, 3 series sections in H. V. arm.
(b) 10:1 divider, 5 series sections in H. V. arm.
(c) 10:1 divider, 7 series sections in H. V. arm.
(d) 200:1 divider, 5 series sections in H. V. arm.

(a)

(b)   GLB-659-4935

Fig. A14. Rise time response of high-voltage resistive divider.
(a) Display of 20-psec-rise pulser on sampling scope having 0.1-nsec
rise time response (0.05 nsec per major division). (b) Signal of 20-psec-
rise pulser passed through 10:1 H. V. resistive divider and displayed on
sampling scope having 0.1-nsec rise time response (0.05 nsec per major
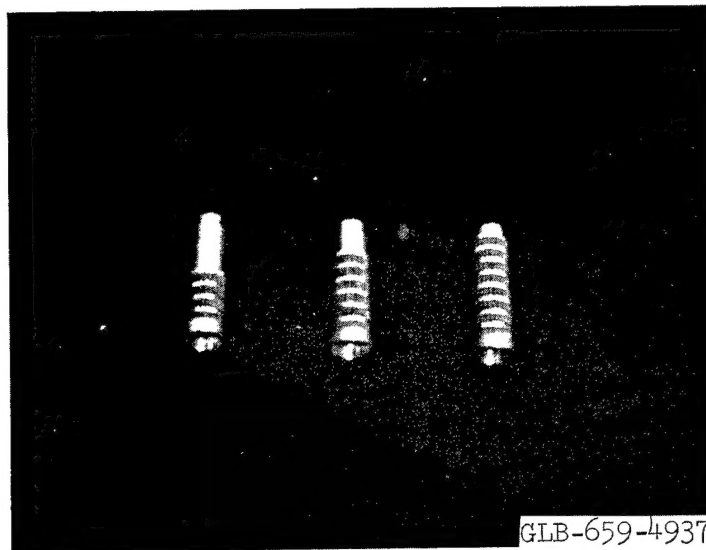division).

GLB-659-4937

Fig. A15. Resistor inserts for high-voltage divider.

A safe upper-pulse voltage limit per resistor section to avoid significant permanent change or damage to resistors was not determined. However, if considerable non-linearity can be tolerated, it is thought that the 1/2 W resistors could be used safely up to 10 kV per resistor section for typical pulse durations of exploding wire circuits.

A very slight permanent decrease in resistance was noticed after about 100 bank discharges at an average stress of 3 to 4 kV per resistor section for a 10-to-1 divider having a seven-section, high-voltage arm.

A resistive divider with seven sections in the high-voltage arm can absorb at least 5 kJ of pulse energy without damage. It was originally thought that current cessations without restrikes might require an appreciable energy dissipation ability by the dividers. However, permanent cessations of chopped current due to wire explosions were never experienced in the tests. Therefore, such energy dissipation capacity would appear not to be essential for the dividers, probably permitting a single string of resistors in a small coaxial enclosure to serve about as well, except that the overall resistance stability feature of many resistors in parallel would be lost.

The coaxial housing for the resistor inserts is comprised of two standard 3-1/8 in.-to-type N coaxial-cable reducers fitted back to back. The type N connector assemblies are removed from the small end extension, and the center-conductor of a short length of RG-213/U is entered at each end of the housing through the type N access which is modified for an O-ring seal. The cable braid is clamped about the type N extension. At the high-voltage input end, the standard teflon-supported 50Ω center-conductor connector portion of the reducer is modified slightly for connection to the center-conductor of the input cable. The center-conductor connector portion of the opposite reducer is dispensed with entirely.

The resistor inserts have "50Ω geometry" brass cylinder extensions on each end for the purpose of fitting into mating cylindrical connections effected by the use of

flexible strip contact soldered circumferentially within the center-conductor connector tube at the high-voltage end and within an appropriate counterbore in the bottom of the opposite reducer to effect the ground connection. The output cable center-conductor connection is made to a crossbar within the cylindrical resistor insert at the top of the output resistor section. The polyethylene-insulated center-conductor of the input cable projects inwardly only about 3/8 in. before an expansion to an effective geometry of 50 Ω characteristic impedance is accomplished by the standard center-conductor connector. The divider assembly is insulated for high voltage with pressurized gas. If it were ever desired to use longer inserts for higher voltages, a standard 3-1/8-in. male-to-male cable adapter housing or similar extension could be interposed between the two end reducers.

The input cable should be kept as short as possible if it is desired to utilize fully the short risetime response capabilities of such a divider, because the high resistance of the divider represents a mismatch to a 50 Ω input cable. In this case, the input cable was about 8 in. in length. Its braid was stripped back a few inches at the input to permit a bolted connection to the exploding wire circuit. The output cable was immediately fitted with a cable connector to feed a 50-nsec length of signal cable to the oscilloscope.

Capacitive dividers feeding a signal cable through a series resistor equal to the characteristic impedance of the cable could be used in place of high-voltage resistive dividers in this scheme if the effective RC time constant of the low-voltage arm is made at least 10 times longer than the longest pulse width to be measured (more, if accuracies better than 10 percent are required). This time constant must be achieved by an appropriate amount of capacitance in the low-voltage arm since the resistor placed in series with the output signal cable must remain equal to the characteristic impedance of the cable. Again, the divider must be placed immediately at the location where voltage is to be measured in order to eliminate reflections in any connection ahead of the divider.

Capacitive dividers are generally not appropriate for as long a pulse-width response at divider ratios as low as existed in this instance. They appear in a more favorable light at considerably shorter pulse widths and higher divider ratios. It might also prove easier to maintain fast risetime response with capacitive dividers at extra high voltages than with resistive dividers.

Compensation Adjustment of Voltage Scheme

A perfectly straight line null adjustment was never achieved in this instance. It is not thoroughly understood why but factors such as the following might be the explanation: (1) imperfect electrostatic shielding of the pickup probe causing a slight polarity offset effect in the probe signal, (2) some resistance drop in the dummy inductance load causing a slight phase shift between the divider signal and the pickup loop signal, (3) stray field coupling to the CRT beam, or (4) a more remote possibility that any voltage induced into the divider by mutual induction might have a slight phase shift compared to the inductive voltage drop across the dummy load.

DISTRIBUTION

	No. of Copies
LRL Internal Distribution,	
Information Division	35
R. J. Thomas	10
J. R. Hearst	10
Carl Rouse	
Gerald L. Johnson	
Gary H. Higgins	
Glenn C. Werth	
Alfred Holzer	
T. R. Butkovich	
R. C. Maninger	
R. W. Kuenning	
C. Ohlson	
E. H. Hulse	
B. D. Faraudo	
R. P. Rossman	
Hyman Olken	3
J. F. Tracy	
A. D. Hyne	
LRL Berkeley,	
R. K. Wakerling, Technical Information	
External Distribution,	
TID-4500 (45th Ed.), UC-37, Instruments	
W. G. Chace, Air Force Cambridge Research Laboratory (CRFA)	
F. D. Bennett, Ballistic Research Laboratories, Aberdeen Proving Ground, Maryland	
E. C. Cnare, Sandia Laboratory, Albuquerque	
Robert Sturgess, Group CMB-7, Los Alamos Scientific Laboratory, Los Alamos, New Mexico	
Kenneth G. Moses, Physics Dept., Temple University, Philadelphia, Penn.	
S. W. Zimmerman, Electrical Eng. Dept., Cornell University, Ithaca, New York	